the plant journal

SEB SOCIETY FOR EXPERIMENTAL BIOLOGY

The Plant Journal (2021) doi: 10.1111/tpj.15242

The BOP-type co-transcriptional regulator NODULE ROOT1 promotes stem secondary growth of the tropical Cannabaceae tree *Parasponia andersonii*

Defeng Shen[1,†], Rens Holmer[1], Olga Kulikova[1], Chanaka Mannapperuma[3], Nathaniel R. Street[3], Zhichun Yan[1], Thomas van der Maden[1], Fengjiao Bu[1], Yuanyuan Zhang[2,‡], Rene Geurts[1,*] and Kévin Magne[1,*,$]

[1]*Laboratory of Molecular Biology, Department of Plant Sciences, Wageningen University & Research, Wageningen 6708 PB, The Netherlands,*

[2]*Laboratory of Plant Physiology, Department of Plant Sciences, Wageningen University & Research, Wageningen 6708 PB, The Netherlands, and*

[3]*Department of Plant Physiology, Umeå Plant Science Centre, Umeå University, Umeå 907 36, Sweden*

Received 14 July 2020; accepted 16 March 2021.

*For correspondence (e-mails: kevin_magne@hotmail.fr and rene.geurts@wur.nl).

[†]Present address: Department of Plant Microbe Interactions, Max Planck Institute for Plant Breeding Research, Cologne, 50829, Germany

[‡]Present address: State Key Laboratory for Conservation and Utilization of Subtropical Agro-bioresources, Guangdong Key Laboratory for Innovative Development and Utilization of Forest Plant Germplasm, College of Forestry and Landscape Architecture, South China Agricultural University, Guangzhou, 510642, China

[$]Present address: Institute of Plant Sciences Paris-Saclay (IPS2), Université Paris-Saclay, CNRS, INRAE, Univ Evry, Orsay, 91405, France

SUMMARY

Tree stems undergo a massive secondary growth in which secondary xylem and phloem tissues arise from the vascular cambium. Vascular cambium activity is driven by endogenous developmental signalling cues and environmental stimuli. Current knowledge regarding the genetic regulation of cambium activity and secondary growth is still far from complete. The tropical Cannabaceae tree *Parasponia andersonii* is a non-legume research model of nitrogen-fixing root nodulation. *Parasponia andersonii* can be transformed efficiently, making it amenable for CRISPR-Cas9-mediated reverse genetics. We considered whether *P. andersonii* also could be used as a complementary research system to investigate tree-related traits, including secondary growth. We established a developmental map of stem secondary growth in *P. andersonii* plantlets. Subsequently, we showed that the expression of the co-transcriptional regulator *PanNODULE ROOT1* (*PanNOOT1*) is essential for controlling this process. *PanNOOT1* is orthologous to *Arabidopsis thaliana BLADE-ON-PETIOLE1* (*AtBOP1*) and *AtBOP2*, which are involved in the meristem-to-organ-boundary maintenance. Moreover, in species forming nitrogen-fixing root nodules, *NOOT1* is known to function as a key nodule identity gene. *Parasponia andersonii* CRISPR-Cas9 loss-of-function *Pannoot1* mutants are altered in the development of the xylem and phloem tissues without apparent disturbance of the cambium organization and size. Transcriptomic analysis showed that the expression of key secondary growth-related genes is significantly down-regulated in *Pannoot1* mutants. This allows us to conclude that PanNOOT1 positively contributes to the regulation of stem secondary growth. Our work also demonstrates that *P. andersonii* can serve as a tree research system.

Keywords: *Parasponia andersonii*, tree, development, vascular cambium, secondary growth, *NOOT-BOP-COCH-LIKE* genes, *NOOT1*.

INTRODUCTION

Mitotic activity of stem cell populations in the shoot apical meristem (SAM) and the root apical meristem (RAM) are responsible for the plant primary growth and enable the plant to grow indefinitely. Plant primary growth is also supported by the presence of a vascular system allowing exchanges along the plant body. In angiosperm and gymnosperm, the primary vasculature is derived from SAM activity and is organized as isolated fascicular bundles interspaced with immature parenchyma surrounding the central pith (Evert and Eichhorn, 2006; Little *et al.*, 2002;

Mazur *et al.,* 2014; Zhu *et al.,* 2018). Primary fascicular bundles consist of vascular stem cells (procambium) from which primary xylem and phloem vascular tissues are generated inward and outward, respectively. To compete for light, plants need to increase their height and consequently strengthen their stems. Many plant species have evolved a developmental process called secondary growth, allowing them to grow radially. During evolution, such a strategy was very successful and, as an example, allowed trees to dominate forest ecosystems.

Secondary growth depends on the vascular cambium (hereafter cambium) activity, a cylindrical sheath of dividing cells within the stem. The cambium originates from fusion of the fascicular procambium and interfascicular cambium. The latter is derived from the transdifferentiation of the interfascicular parenchyma cells (Barnett, 1981; Fischer *et al.,* 2019; Helariutta and Bhalerao, 2003; Johnsson and Fischer, 2016; Larson, 1994; Mellerowicz *et al.,* 2001; Miyashima *et al.,* 2013; Nieminen *et al.,* 2015). The cambium produces secondary xylem (wood) inward and secondary phloem (bast) outward (Evert and Eichhorn, 2006).

The activity of cambium responds to environmental and mechanical stimuli and is controlled by phytohormones and signaling peptides. Most phytohormones appear to play promotive roles in the regulation of cambium and secondary growth (Brackmann and Greb, 2014; Campbell and Turner, 2017; Fischer *et al.,* 2019; Miyashima *et al.,* 2013; Ragni and Greb, 2018). Cambium stem cell proliferation is also controlled by the peptide-receptor-transcription factor module TRACHEARY ELEMENT DIFFERENTIATION INHIBITORY FACTOR (TDIF) — PHLOEM INTERCALATED WITH XYLEM TDIF RECEPTOR (PXY-TDR) — WUSCHEL-RELATED HOMEOBOX 4 (WOX4). In the cambium, the type-B TDIF peptides CLE41 and CLE44 bind the receptor PXY-TDR and induce the expression of the transcription factor *WOX4*. WOX4 inhibits xylem cell identity acquisition and allows the proper delimitation, orientation and promotion of cambium proliferation (Etchells *et al.,* 2013, 2015; Etchells and Turner, 2010; Fisher and Turner, 2007; Hirakawa *et al.,* 2010; Hirakawa *et al.,* 2008; Immanen *et al.,* 2016; Ito *et al.,* 2006; Ji *et al.,* 2010; Kucukoglu *et al.,* 2017; Liu *et al.,* 2016; Nilsson *et al.,* 2008; Schrader *et al.,* 2004; Suer *et al.,* 2011; Tuominen *et al.,* 1997; Whitford *et al.,* 2008; Zhu *et al.,* 2019). Besides PXY-TDR, other receptors also contribute to cambium regulation. The SOMATIC EMBRYOGENESIS RECEPTOR KINASEs (SERKs) function as PXY-TDR co-receptors (Zhang *et al.,* 2016), whereas the PXY-TDR homologous receptors PXY-LIKE1 (PXL1) and PXL2 function synergistically to regulate vascular tissue development in the stem (Etchells *et al.,* 2013; Fisher and Turner, 2007). Furthermore, REDUCED IN LATERAL GROWTH1 (RUL1) and MORE LATERAL GROWTH1 (MOL1) control cambium homeostasis (Agusti *et al.,* 2011; Gursanscky *et al.,* 2016) and the receptor-kinases ERECTA (ER) and ERECTA-LIKE1 (ERL1) redundantly control secondary growth by preventing premature initiation of xylem fibre differentiation in the hypocotyl (Ikematsu *et al.,* 2017). Taken together, these studies highlight the importance of hormonal and peptide signaling modules in the regulation of cambium formation and activity.

Current knowledge regarding cambium and secondary growth genetic regulation is under progress but is still far from complete. Most studies have been conducted using either *Populus* species, *Populus* hybrids or the herbaceous model *Arabidopsis thaliana*. We considered whether we could use *Parasponia andersonii* as a complementary research system to obtain novel insights into the genetic regulation of secondary growth. *Parasponia andersonii* is a fast growing tree, for which efficient transformation protocols and a sequenced and annotated genome are available (van Velzen *et al.,* 2018; Wardhani *et al.,* 2019; van Zeijl *et al.,* 2018). The *Parasponia* lineage represents five perennial evergreen tropical tree species that are native to the Malay Archipelago (Becking, 1992). The *Parasponia* lineage is part of the larger *Trema* genus, which belongs to the Cannabis family (Cannabaceae; order Rosales) (van Velzen *et al.,* 2018; Yang *et al.,* 2013). Cannabaceae includes ten genera and approximately 180 species consisting mostly of trees and shrubs (Yang *et al.,* 2013). *Parasponia* and *Trema* species are pioneer plants with similar growth characteristics that thrive well on poor soils. Especially, *Parasponia* can colonize harsh landscapes post-volcano eruptions (Ishaq *et al.,* 2020). Also, *Parasponia* species are the only non-leguminous plants that have the capacity to establish root nodules with diazotrophic rhizobia, making it an important comparative research system for investigating the evolution of this trait (Behm *et al.,* 2014; van Velzen *et al.,* 2018). *Parasponia* can grow up to 6 m a year, similar to that reported for *Trema orientalis*, which is also known as Nalita (Jahan and Mun, 2003; Trinick, 1980). Nalita wood is diffuse and porous and is considered as an alternative source of fiber for pulp production in the paper industry (Jahan and Mun, 2003; Jahan *et al.,* 2007, 2010).

Parasponia andersonii possesses significant advantages for applying reverse genetic studies, especially in the context of tree development. Its genome is relatively small (563 Mbp) and has a high level of homozygosity (Holmer *et al.,* 2019; van Velzen *et al.,* 2018). *Parasponia andersonii* did not experience a recent whole genome duplication, as is the case in Salicoid, and, consequently, cases of gene redundancy are rare compared to more traditional model trees such as *Populus* species or *Populus* hybrids (Brunner *et al.,* 2000; Tuskan *et al.,* 2006). Besides, *P. andersonii* benefits from *in vitro* propagation and rooting procedures, from an efficient transformation procedure taking 2–3 months (transformation rate > 50%) and from an effective CRISPR-Cas9 (Clustered Regularly Interspaced Short Palindromic Repeats/CRISPR-associated protein 9) genome

editing strategy allowing the generation of biallelic recessive mutants (Bu *et al.,* 2020; Rutten *et al.,* 2020; van Velzen *et al.,* 2018; Wardhani *et al.,* 2019; van Zeijl *et al.,* 2018). Moreover, *P. andersonii* reaches its sexual maturity within 5 months and seeds remain viable for years (Becking, 1992). Its genetic assets coupled with its dedicated toolbox make *P. andersonii* particularly suitable for the investigation of tree development via reverse genetic approach, and the availability of viable seeds enables the investigation of early tree developmental phases.

The *NODULE ROOT* (*NOOT*) — *BLADE-ON-PETIOLE* (*BOP*) — *COCHLEATA* (*COCH*) — *LIKE* genes (*NBCL*, also known as *BOP-LIKE*) are plant specific developmental regulators encoding BTB/POZ (BROAD-COMPLEX, TRAMTRACK and BRICK-A-BRACK/POXVIRUS and ZINC FINGER) and ANKYRIN domain repeats proteins (Couzigou *et al.,* 2012). *NBCL* genes encode co-transcriptional regulators that can also act as E3 ubiquitin ligase adapters regulating protein homeostasis (Jun *et al.,* 2010; Zhang *et al.,* 2017). NBCLs are conserved in both dicots and monocots, and were shown to be involved in a myriad of developmental processes (Dong *et al.,* 2017; Hepworth and Pautot, 2015; Jost *et al.,* 2016; Khan *et al.,* 2014; Magne *et al.,* 2020; Tavakol *et al.,* 2015; Toriba *et al.,* 2019; Wang *et al.,* 2016). NBCL proteins are involved in boundary formation. These specific domains are important for partitioning meristematic domains from lateral organs (Aida and Tasaka, 2006a, 2006b; Barton, 2010; Zadnikova and Simon, 2014). In line with this, we hypothesized that *NBCL* genes are also critical for stem secondary growth. However, such functioning has never been reported.

In the present study, our objectives were two-fold. First, we aimed to determine whether *P. andersonii* could be used as a tree research system. Second, we aimed to determine whether *NBCL* genes contribute to stem secondary growth. To achieve these objectives, we investigated the function of the single *NBCL* gene of *P. andersonii*, namely *PanNODULE ROOT1* (*PanNOOT1*), during stem secondary growth. To do so, a stem secondary growth developmental map was created and combined with the gene expression profiles of key secondary growth regulators. *PanNOOT1* displayed a complementary expression profile compared to secondary growth regulators, suggesting an antagonistic function during cambium initiation. Subsequent knockout mutagenesis of *PanNOOT1* demonstrated that PanNOOT1 is an essential component of the stem secondary growth regulation.

RESULTS

A developmental map of cambium formation in *P. andersonii*

The establishment of cambium marks the transition from a juvenile stem towards a mature and fully functional stem. Once fascicular and interfascicular cambia merge and form a complete cambium ring, stem secondary growth starts and both secondary xylem and phloem tissues accumulate. Because of a lack of information regarding the dynamics of cambium formation in *P. andersonii*, we investigated this developmental process using the *P. andersonii* wild-type reference genotype WU1-14 (*Pan*WU1-14) (Op den Camp *et al.,* 2011; van Velzen *et al.,* 2018). To determine the dynamics of cambium formation in *P. andersonii*, an epicotyl developmental map was created using *in vitro* grown seedlings. Transversal sections of the first internode above the cotyledons (epicotyl) were histologically analyzed from plantlets after 13, 15, 18, 22, 26, 30, 35 and 42 days post-germination (Figure 1). From 13 to 22 days, *P. andersonii* epicotyl vascular elements were organized as distinct poles. At these stages, vascular poles consisted of xylem and phloem tissues developing inward and outward from the fascicular cambium, respectively (Figure 1, panels 1–16). At 22 days, periclinal divisions initiated in the interfascicular parenchyma adjacent to the fascicular bundles. We noted that these cell divisions tended to occur synchronously in the different interfascicular parenchyma regions. These observations indicated that the interfascicular cambium started to establish (Figure 1, panels 13–16). At this stage, *in vitro* grown *P. andersonii* plantlets harboured four developed leaves and started to develop a fifth one (Figure S1). From day 26, the cambium was fully established, forming a complete ring of dividing cells. Once the cambium of *P. andersonii* epicotyl is established, xylogenesis occurs rapidly. Secondary xylem and phloem tissues accumulated inward and outward from the cambium, respectively (Figure 1, panels 17–32). Therefore, we concluded that, for *in vitro* grown *P. andersonii* seedlings, cambium formation starts at 22 days post-germination, as a synchronized process. Ultimately, the structure of the wood in *P. andersonii* epicotyl is typical and consists of the regular angiosperm wood elements such as xylem fibres and xylem vessels regularly interspaced with xylem rays.

The expression of secondary growth developmental marker genes correlates with the dynamics of cambium formation

We considered whether the dynamics of *P. andersonii* secondary growth correlated with the transcriptional activation of cambium, xylem and phloem developmental marker genes. To identify such marker genes in *P. andersonii,* we used inferred orthogroup data available for *P. andersonii*, *Populus trichocarpa, Eucalyptus grandis* and *A. thaliana* and determined orthologous gene relation for known secondary growth marker genes (Emms and Kelly, 2015; van Velzen *et al.,* 2018). In addition, we included other *Populus* species in our analysis. We identified 67 orthogroups that contained genes known to be involved in secondary growth, representing 90 genes in *P. andersonii*,

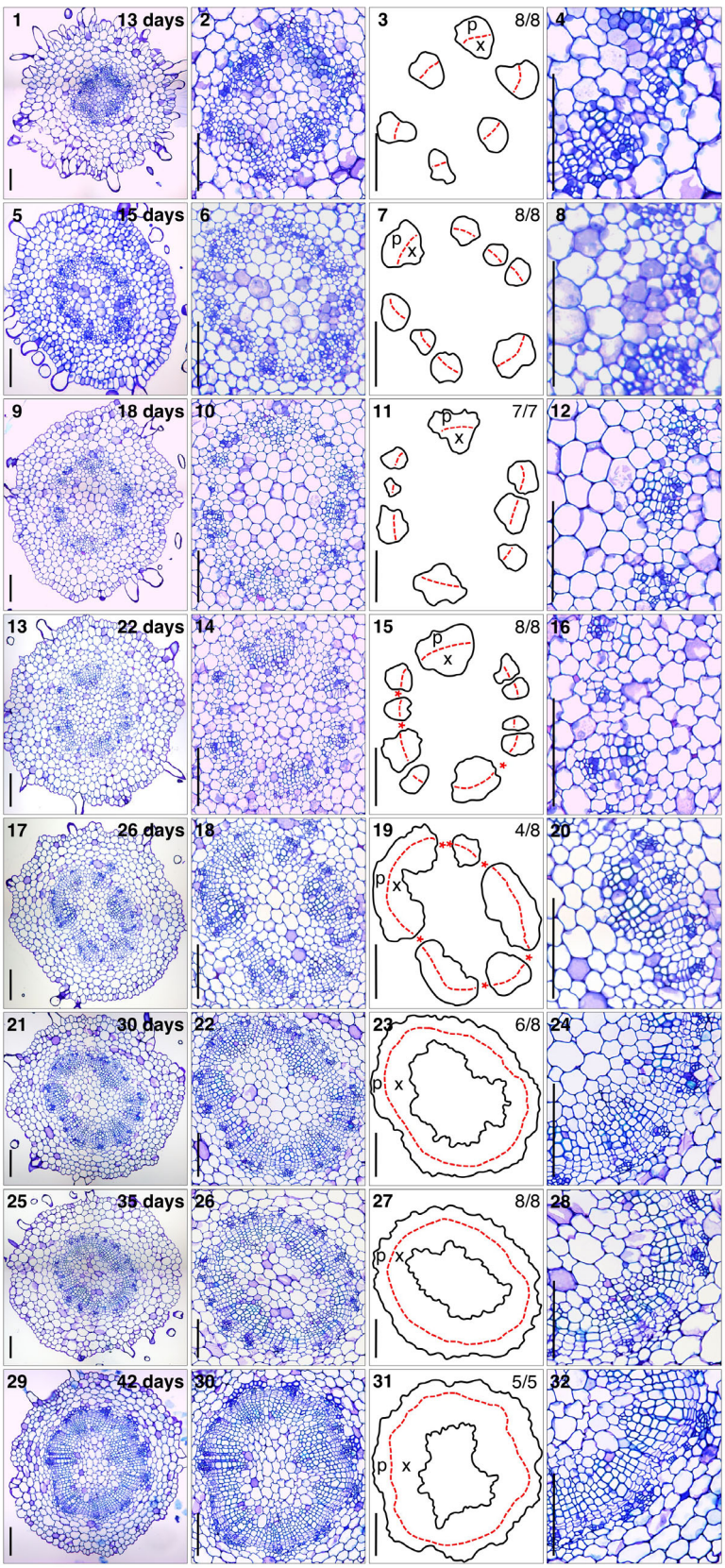

Figure 1. Developmental kinetics of *P. andersonii* vascular cambium establishment. Transversal sections of the first internode above cotyledons (epicotyl) of *in vitro* grown *P. andersonii* seedlings of genotype *Pan*WU1-14 at 13, 15, 18, 22, 26, 30, 35 and 42 days post-germination. The first column shows entire epicotyl transversal sections. The second column shows magnifications focusing on vascular tissues organization. The third column provides simplified schemes of the vascular tissue organization generated from images in the second column . The fourth column shows magnifications focusing on the cambial zone. Panels 1–16, from 13 to 22 days, *Pan*WU1-14 epicotyl vascular elements are organized as isolated poles. Each vascular pole consists of xylem and phloem tissues developing inward and outward from the procambium (red dotted-lines), respectively. Panels 13–16, At 22 days post-germination, the first interfascicular cambium cell divisions occur (red asterisks). Panels 17–32, from 26 to 42 days, *Pan*WU1-14 epicotyl transversal sections display a complete ring of cambial cells (red dotted-lines) with xylem and phloem accumulating inward and outward from the cambium respectively. p, phloem tissues; x, xylem tissues; red dotted-lines, vascular cambium; red asterisks, interfascicular cambium cell divisions. Ratios in schemes of the right column indicate the number of transversal sections showing identical vascular tissues organization. Thickness = 7 μm. Scale bars = 100 μm

159 genes in *P. trichocarpa*, 140 genes in *Populus tremula*, 144 genes in *Populus alba*, 121 genes in *E. grandis* and 109 genes in *A. thaliana* (Table S1). Subsequently, the *P. andersonii* orthologs of known secondary growth marker genes were identified by additional and reciprocal BLAST (Basic Local Alignment Search Tool) analysis between *P. andersonii, A. thaliana* and *P. trichocarpa*, as well as by phylogenetic reconstruction analysis (Dataset S1). The *P. andersonii* genome was shown to contain direct orthologs for all secondary growth-related genes tested here, except for one, *XYLEM CYSTEINE PEPTIDASE2* (*XCP2*). Collectively, this suggests that the *P. andersonii* lineage is less prone for gene duplications compared to the *Populus* genus.

Following the identification of *P. andersonii* secondary growth-related orthologous genes, gene expression profiling was performed for key secondary growth markers with epicotyl samples from 13, 15, 18, 22, 26, 30, 35 and 42 days post-germination plantlets that were used to establish the cambium developmental map of *P. andersonii*. First, gene expression profiles were generated for the *P. andersonii* genes *PanCLE41, PanPXY-TDR, PanWOX4* and *PanMOL1* regulating cambium activity (Figure 2a; Table S1; Dataset S1). Quantitative real-time polymerase chain reaction (qRT-PCR) analysis revealed that these four cambium activity marker genes were simultaneously induced in the epicotyl at 22 days post-germination, concomitantly with the first interfascicular cambium cell divisions (Figure 1, panels 13–16; Figure 2a). *PanCLE41*, *PanPXY-TDR*, *PanWOX4* and *PanMOL1* expression continued to increase until 26 days post-germination and then remained stable (Figure 2a).

In *P. tremula* and the hybrid *P. tremula* × *P. alba,* class I *KNOTTED1-LIKE HOMEOBOX* (class I *KNOX*) genes promote cambium activity and regulate cambium daughter cell differentiation (Du *et al.,* 2009; Groover *et al.,* 2006; Schrader *et al.,* 2004). We thus investigated the expression of the *P. andersonii* class I *KNOX* genes *PanSTM1* and *PanSTM2*, orthologous to *A. thaliana SHOOT MERISTEMLESS* (*AtSTM*) and *P. tremula* × *P. alba ARBORNOX1* (*ARK1,* Groover *et al.,* 2006), as well as *PanBP,* orthologous to *A. thaliana BREVIPEDICELLUS* (*AtBP*) and *P. tremula* × *P. alba ARBORNOX2* (*ARK2,* Du *et al.,* 2009) (Figure 2b; Table S1; Dataset S1). *PanSTM1*, *PanSTM2* and *PanBP* gene expression profiles were highly similar and induced in the epicotyl from 22 days post-germination when interfascicular cambium starts to form (Figure 1, panels 13–16; Figure 2b). *PanSTM1*, *PanSTM2* and *PanBP* expression continued to increase until 30 days post-germination. At this stage, the cambium was fully developed (Figure 1, panels 21–24; Figure 2b). Then, from day 30 to 42, the expression of these three class I *KNOX* genes tended to decrease.

Together, these seven cambium marker genes showed a similar expression profile and were simultaneously up-regulated in the epicotyl of 22-day-old plants concomitantly with the initiation of the cambium establishment. This suggests that, in *P. andersonii,* these genes might also represent regulators of cambium initiation and functioning. The finding that the expression of these genes in the epicotyl reaches a plateau at approxmately 26 days post-germination indicates that, once the cambium is established, cambium activity reaches an equilibrium.

We next investigated the gene expression profiles of the key xylem and phloem developmental markers *PanSND1, PanNST1, PanVND6, PanCNA* and *PanAPL*, which are, respectively, orthologous to the *A. thaliana* SECONDARY WALL-ASSOCIATED NAC-DOMAIN PROTEIN 1 (AtSND1) and NAC SECONDARY WALL THICKENING PROMOTING FACTOR 1 (AtNST1) promoting xylem fibre differentiation and secondary cell wall thickening (Mitsuda *et al.,* 2007; Zhong *et al.,* 2006), to the *A. thaliana* VASCULAR-RELATED NAC-DOMAIN 6 (AtVND6), a master regulator of xylem differentiation (Kubo *et al.,* 2005; Ohashi-Ito *et al.,* 2010; Yamaguchi *et al.,* 2010), to the class III HD-ZIP transcription factor CORONA (CNA) involved in xylem development and tracheary elements differentiation (Carlsbecker *et al.,* 2010; Du *et al.,* 2011; Ilegems *et al.,* 2010; Prigge *et al.,* 2005), and to the MYB coiled-coil-type transcription factor, ALTERED PHLOEM DEVELOPMENT (AtAPL), required for phloem identity acquisition, phloem differentiation and xylem identity inhibition in phloem (Bonke *et al.,* 2003) (Figure 2c; Table S1; Dataset S1). qRT-PCR analysis showed that these xylem and phloem developmental marker genes were also induced during *P. andersonii* secondary growth. The expression of these genes was sequentially up-regulated and showed a maximum expression at approximately 30–35 days post-germination, after which expression levels started to decrease. *PanSND1* was among the earliest induced marker genes, detectable in the epicotyl at 15 days post-germination. By contrast, *PanVND6* and *PanAPL* were induced from 22 days post-germination and, finally, *PanCNA* and *PanNST1* were only induced from day 26 onwards. Although *PanVND6*, *PanAPL* and *PanCNA* showed similar maximum expression levels, between 2- to 4-fold changes, *PanSND1* and *PanNST1* showed higher maximum expression levels, with between 16- and 64-fold changes, respectively (Figure 2c).

In conclusion, all of the *P. andersonii* orthologs of cambium, xylem and phloem developmental marker genes identified in *Populus* species and/or *A. thaliana* were induced during *P. andersonii* secondary growth. The expression profiles of the different marker genes that we investigated were correlated with the developmental dynamics of *P. andersonii* secondary growth.

The *NBCL* gene *PanNODULE ROOT1* is down-regulated during cambium initiation but expressed in xylem, cambial and phloem tissues during secondary growth

Studies in *A. thaliana* have shown that the class I KNOX transcription factors AtSTM and AtBP repress the

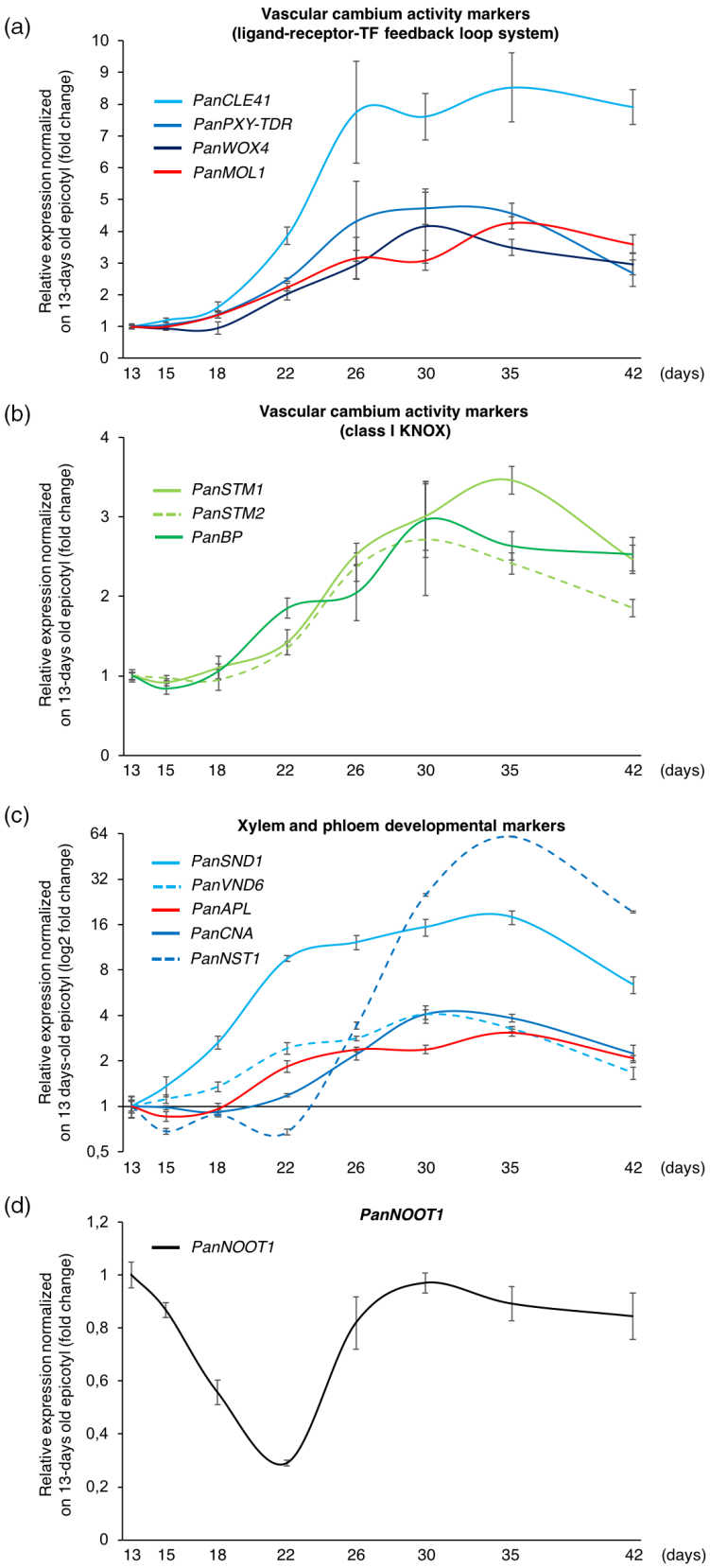

Figure 2. *PanNOOT1* gene expression profile compared to vascular cambium, xylem and phloem marker gene expression profiles during *P. andersonii* stem secondary growth kinetics.
(a–d) qRT-PCR gene expression profile of *PanNOOT1* gene compared to vascular cambium, xylem and phloem developmental markers during the kinetic of *P. andersonii* stem secondary growth described in Figure 1. qRT-PCR gene expression analysis was performed on the first internode above cotyledons (epicotyl) from *in vitro* grown *P. andersonii* plants at 13, 15, 18, 22, 26, 30, 35 and 42 days. *Parasponia andersonii* vascular cambium, xylem and phloem marker genes represent orthologs of vascular cambium, xylem and phloem marker genes described in *A. thaliana* and/or in *Populus* sp. (Table S1 and Dataset S1). (a) qRT-PCR gene expression analysis of *PanCLE41* (light blue curve), *PanPXY-TDR* (blue curve) and *PanWOX4* (dark blue curve) involved in the ligand-receptor-TF feedback loop systems regulating vascular cambium stem cell maintenance. qRT-PCR gene expression analysis of *PanMOL1* (red curve) involved in the regulation of interfascicular cambium cell proliferation. (b) qRT-PCR gene expression analysis of the class I *KNOX* transcription factor genes *PanSTM1* (light green curve), *PanSTM2* (light green dotted curve) and *PanBP* (green curve) involved in vascular cambium stem cell maintenance. (c) qRT-PCR gene expression analysis of *PanSND1* (light blue curve), *PanVND6* (light blue dotted curve), *PanCNA* (blue curve) and *PanNST1* (blue dotted-curve) involved in xylem development. qRT-PCR gene expression analysis of *PanAPL* (red curve) involved in phloem development. d, qRT-PCR gene expression analysis of *PanNOOT1* (black curve). (a–d) Gene expression data were normalized against the constitutively expressed *PanELONGATION FACTOR1α* (*PanEF1α*) gene as well as against the expression levels from 13-day-old reference samples. (a, b and d) The *y*-axis represents fold changes. (c) The *y*-axis represents log2 (fold changes). Results represent thre mean ± sem from three biological replicates. Gene abbreviations: *PanCLE41, PanCLAVATA3/ESR-RELATED41* (*PanWU01x14_078150*); *PanPXY-TDR, PanPHLOEM INTERCALATED WITH XYLEM-TDIF RECEPTOR* (*PanWU01x14_218900*); *PanWOX4, PanWUSCHEL RELATED HOMEOBOX4* (*PanWU01x14_119590*); *PanMOL1, PanMORE LATERAL GROWTH1* (*PanWU01x14_105020*); *PanSTM1, PanSHOOT MERISTEMLESS1* (*PanWU01x14_211410*); *PanSTM2, PanSHOOT MERISTEMLESS2* (*PanWU01x14_287890*); *PanBP, PanBREVIPEDICELLUS* (*PanWU01x14_033300*); *PanSND1, PanSECONDARY WALL-ASSOCIATED NAC DOMAIN1* (*PanWU01x14_056920*); *PanVND6, PanVASCULAR-RELATED NAC-DOMAIN6* (*PanWU01x14_182640*); *PanAPL, PanALTERED PHLOEM DEVELOPMENT* (*PanWU01x14_155850*); *PanCNA, PanCORONA* (*PanWU01x14_195660*); *PanNST1, PanNAC SECONDARY WALL THICKENING PROMOTING FACTOR1* (*PanWU01x14_041300*); *PanNOOT1, PanNODULE ROOT1* (*PanWU01x14_292800*)

expression of the *NBCL* genes *AtBOP1* and *AtBOP2* to allow xylem fibre differentiation and vessel formation during root thickening (Liebsch *et al.,* 2014; Woerlen *et al.,* 2017). Available *P. andersonii* transcriptomic data showed that the *AtBOP1-AtBOP2* orthologous gene *PanNOOT1* is expressed in several organs, including the stem (Figure S2) (van Velzen *et al.,* 2018; www.parasponia.org). To confirm the presence of *PanNOOT1* transcripts in *P. andersonii* stem and to determine the expression profile of *PanNOOT1* during the establishment of the cambium, qRT-PCR were performed on the RNA extracted from the epicotyl samples corresponding to the secondary growth kinetic studies (Figure 1). This revealed that *PanNOOT1* displayed a characteristic expression profile in the developing epicotyl (Figure 2d). From 15 to 22 days, prior to the first interfascicular cambium cell divisions, the expression of *PanNOOT1* fell drastically and decreased by 71% at 22 days. Then, from 22 days, the expression increased and reached a stable expression level from 30 days onwards, coinciding with a fully developed and functional cambium (Figure 2d). This indicates that the expression profiles of *PanNOOT1* and cambium activity gene markers are complementary, suggesting antagonistic functions during cambium initiation (Figure 2). It is also suggested that molecular mechanisms involving the repression of *PanNOOT1* by class I KNOX transcription factors might be conserved in tree species for the control of cambium initiation and functioning.

To determine the spatial expression pattern of *PanNOOT1* in *P. andersonii* stem, we performed *in situ* hybridization (ISH) using the *PanNOOT1* probe sets from Shen *et al.,* 2020 and investigated transgenic *P. andersonii* lines expressing a *PanNOOT1* promoter GUS reporter construct (*promPanNOOT1:GUS:PanNOOT1ter*). Because transgenic *P. andersonii* lines are maintained clonally (Wardhani *et al.,* 2019) and because *in vitro* propagated plantlets grew less synchronized compared to seedlings, we investigared *PanNOOT1* spatial expression in 7–10-week-old plants and analyzed the second and third fully elongated internodes, counted from the shoot apical meristem. Using both approaches, the expression of *PanNOOT1* was detected in phloem parenchyma, in cambial zone, in differentiating secondary xylem cells, in differentiated secondary xylem fibres and in the older primary xylem, whereas it was not detected in cortex, in phloem sclerenchyma, in phloem sieve elements and in xylem vessels (Figure 3; Figure S3). ISH and promoter GUS reporter fusion approaches showed redundant spatial expression profiles, indicating that the 3.385 kb region upstream of *PanNOOT1* may represent functional promoter elements. These results suggest that *PanNOOT1* might play a role in the regulation of phloem, cambial and xylem tissues development.

The loss-of-function of *PanNOOT1* alters stem secondary growth

To determine whether *PanNOOT1* has a critical role in *P. andersonii* stem secondary growth, CRISPR-Cas9 loss-of-function mutants were generated. Using three guide RNAs that target the first exon of the *PanNOOT1* gene, three independent mutant lines were identified (*Pannoot1 A5*, *A10* and *A29*). All three *Pannoot1* mutant lines presented a homozygous single nucleotide mutation at base pair 36 of the coding region, which is covered by guide RNA 1. Additionally, all three lines presented a second and wider deletion that varies in size, being either homozygous or biallelic (Figure S4). In all cases, this caused premature stop codons in the *PanNOOT1* open reading frame. The *Pannoot1 A5* and *A10* alleles may encode a 26 amino acid truncated protein, whereas, in the case of the *Pannoot1 A29* allele, the putatively encoded truncated protein has a length of 18 amino acids (Figure S4). This allowed us to consider *Pannoot1 A5*, *A10* and *A29* as knockout mutants.

To determine the consequences of the loss-of-function of *PanNOOT1* on *P. andersonii* stem secondary growth, *Pannoot1 A5*, *A10* and *A29* internode diameters were compared with the wild-type line *Pan*WU1-14 and the transgenic control line *PanCtr-44* (van Zeijl *et al.,* 2018). However, the *Pannoot1* mutants presented a very strong alteration of axillary shoot outgrowth (Figure S5; Shen *et al.*, unpublished data). Such a strong developmental defect might impact the photosynthetic rate, as well as secondary growth, and therefore could generate a bias in our interpretation. To ascertain that the *Pannoot1* secondary growth phenotype is a result of the loss-of-function of *PanNOOT1* rather than to a lack of axillary shoots, we included additional controls consisting of *Pan*WU1-14 and *PanCtr-44* plants manually trimmed for their axillary shoots since their seedling stage (hereafter, trimmed *Pan*WU1-14 and trimmed *PanCtr-44*). Plant genotypes were grown for 10 weeks under greenhouse conditions (28°C, 85% relative humidity), resulting in plants with approximately 10 internodes [numbered here from most basal internode (IN1) to upper internode (IN10)]. At this stage of development, we noted that basal internodes produced cork, an outermost stem-protective tissue also called periderm (Figure S5), and we showed that *P. andersonii* developed a cork cambium also called phellogen (Figure S6). In upper internodes, from IN6 to IN10, trimmed *Pan*WU1-14 and *PanCtr-44* had significantly larger internode diameters compared to untrimmed *Pan*WU1-14 and *PanCtr-44* plants (Figure 4). This suggests that the absence of axillary shoots led to an increased secondary growth in the youngest internodes. However, this phenotype was not observed in *Pannoot1* mutants, despite the absence of lateral branch outgrowth. By contrast, in the basal internodes, from IN1 to IN4, the diameter of internode of *Pannoot1 A5*, *A10* and *A29* mutant

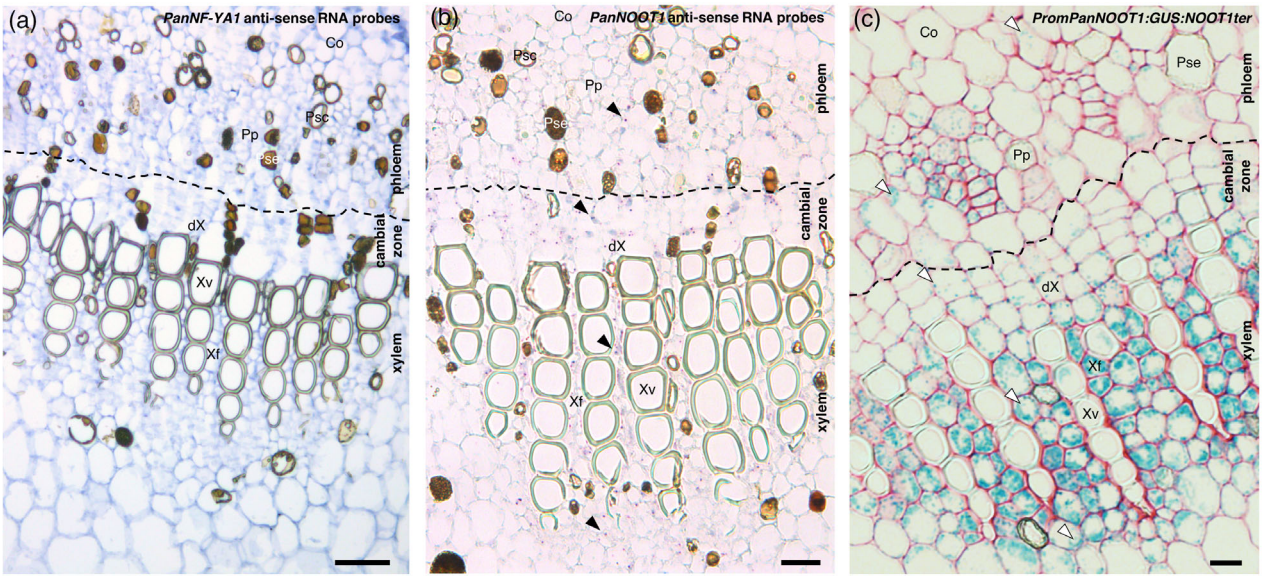

Figure 3. *PanNOOT1 in situ* RNA hybridization and *promoter GUS* expression patterns in *P. andersonii* stem. The expression pattern of *PanNOOT1* was determined by *in situ* hybridization and using transgenic lines expressing a *PromPanNOOT1:GUS:NOOT1ter* fusion.
(a,b) *In situ* hybridizations were performed on cross sections of the second fully elongated internode from the shoot apex of 10-week-old *P. andersonii Pan*WU1-14 plants. (a) Anti-sense RNA probes targeting the nodule-specific *PanNF-YA1* mRNAs (*PanWU01x14_284830*) served as negative control (Bu et al., 2020). No specific expression pattern or signal background were observed for *PanNF-YA1*. (b) Specific *PanNOOT1* anti-sense RNA probes (red signals indicated by black arrowheads) were detected in phloem parenchyma, in cambial zone, in differentiating secondary xylem cells, in secondary xylem fibres and in the older primary xylem. Signals were not detected in cortex, in phloem sclerenchyma and sieve elements, nor in xylem vessels. (c) *PanNOOT1* gene expression pattern in the third fully elongated internode from the shoot apex of 7-week-old *P. andersonii Pan*WU1-14 stable transformants expressing the GUS reporter fusion *PromPanNOOT1:GUS:NOOT1ter*. The X-gluc staining (blue coloration indicated by white arrowheads) was detected in phloem parenchyma, in cambial zone, in differentiating secondary xylem cells, in secondary xylem fibres and in the older primary xylem. Signals were not detected in cortex, in phloem sclerenchyma and sieve elements, nor in xylem vessels. Black dotted lines indicate the frontier between the cambial zone and the phloem tissues. Co, cortex; Psc, phloem sclerenchyma; Pp, phloem parenchyma; Pse, phloem sieve elements; dX, differentiating xylem; Xf, xylem fibres; Xv, xylem vessels. Thickness: (a,b) 6 μm; (c) 7 μm. Scale bar: (a) 50 μm; (b,c) 25 μm

plants were significantly reduced compared to all trimmed and untrimmed control plants (Figure 4). The reduced secondary growth phenotype of *Pannoot1* was also observed in older plants that were analyzed 20 weeks post-planting. Of the five most basal internodes, the diameters of *Pannoot1 A5* were significantly reduced relative to *Pan*WU1-14 (Figure S7). These results indicated that the loss-of-function of *PanNOOT1* negatively affects *P. andersonii* stem secondary growth in an axillary shoot-independent manner.

To understand why the *Pannoot1* mutant stems were thinner, hand sections of the most basal internodes from all genotypes were made and the whole stem, the xylem and the phloem tissues areas were measured. Whole stem, xylem and phloem areas were significantly reduced in the three *Pannoot1* mutants compared to all of the control plants (Figure S8). These results indicated that the reduced secondary growth observed in *Pannoot1* is caused by a reduction of both xylem and phloem tissues development. This might be either the result of a reduction of cell size and/or a reduction of the number of cell layers. To determine why xylem and phloem surfaces were reduced in *Pannoot1* mutants, and to characterize the *Pannoot1* stem tissues organization, thin resin sections were obtained from the most basal internodes of 10-week-old plants. Figure 5 shows representative sections indicating the reduced secondary growth in *Pannoot1 A5*, *A10* and *A29* compared to the different controls . Besides the apparent secondary growth reduction occurring in *Pannoot1* mutants, the organization of the *Pannoot1* stem tissues did not differ from control plants. All genotypes showed a wild-type tissue organization consisting of a central pith, sequentially surrounded by the xylem, the cambial zone, the phloem, the cortex and the periderm (Figure 5). Based on resin sections, secondary growth developmental parameters were defined and assessed in detail. In *Pannoot1* mutants, the size of the cambium cells, the number of cell layers present in the cambial zone and the size of the first thickened xylem fibre cells were not significantly different compared to the control plants (Figure 5h, i, j). However, the number of differentiated xylem cell layers (Figure 5k) and the size of the differentiated xylem vessels were significantly reduced in *Pannoot1* mutants (Figure 5l). This suggests that the formation and the differentiation of the xylem cells is affected in *Pannoot1* mutants. In addition, at the phloem side, histological analysis revealed a reduced number of

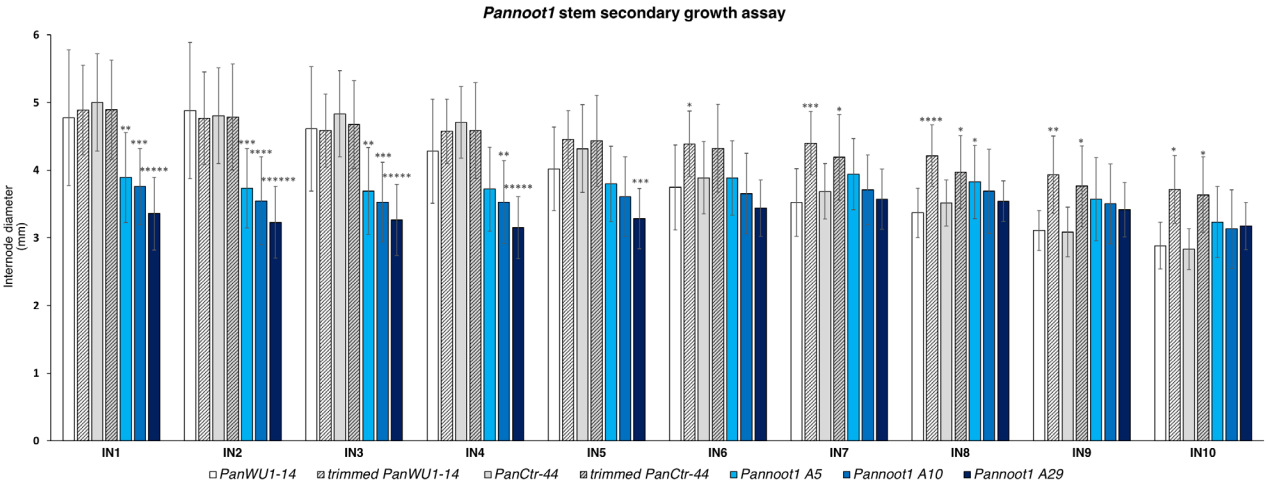

Figure 4. *Parasponia andersonii Pannoot1* mutants present a reduced stem secondary growth. Measurement of stem diameters in *Pannoot1 A5* (light blue bars), *Pannoot1 A10* (blue bars) and *Pannoot1 A29* (dark blue bars) compared to wild-type *Pan*WU1-14 (white bars), trimmed wild-type *Pan*WU1-14 (hatched white bars), transgenic control *PanCtr-44* (grey bars) and trimmed transgenic control *PanCtr-44* (hatched grey bars). Stem diameters were measured at the middle of internodes (IN) for the first 10 internodes, from the bottom to the top of 10-week-old plants. For *Pan*WU1-14, trimmed *Pan*WU1-14, *PanCtr-44*, trimmed *PanCtr-44*, *Pannoot1 A5*, *Pannoot1 A10* and *Pannoot1 A29*, n = 15, 15, 15, 15, 30, 30 and 26 plants, respectively. Error bars represent the SD. Asterisks indicate significant differences relative to wild-type *Pan*WU1-14 (*$P < 1 \times 10^{-2}$; **$P < 1 \times 10^{-3}$; ***$P < 1 \times 10^{-4}$; ****$P < 1 \times 10^{-5}$; *****$P < 1 \times 10^{-6}$; ******$P < 1 \times 10^{-7}$; Student's *t*-test)

phloem cell layers in *Pannoot1* mutants compared to the control plants (Figure 5m).

Despite cambial zone integrity and organization apparently not being affected in *P. andersonii Pannoot1* mutant lines, we showed that the reduced secondary growth phenotype observed in these mutants is the result of a reduced number of cell layers in both xylem and phloem tissues. These results suggest that, in the stem of *P. andersonii*, PanNOOT1 promotes both xylem and phloem tissues development.

The loss-of-function of *PanNOOT1* affects the expression of secondary growth-related genes

Because AtBOP1 and AtBOP2 act as co-transcriptional regulators in *A. thaliana*, we considered to what extent the loss-of-function of *PanNOOT1* can affect gene expression in *P. andersonii* internodes. To identify and quantify the transcriptional role of PanNOOT1 in *P. andersonii* internodes, we focused on the first three fully elongated internodes (*fe*lN1, *fe*lN2 and *fe*lN3) from the shoot apex of 8-week-old plants. Histological analysis revealed that, in *fe*lN1, *fe*lN2 and *fe*lN3, the cambium was fully established and that internodes underwent secondary growth. In these young internodes, no significant phenotypic differences were observed between *Pannoot1* mutant alleles and control plants (Figure S9). Because of their developmental resemblance, these *Pannoot1 A5*, *A10* and *PanCtr-44* internode samples were chosen for RNA sequencing (RNA-seq) approaches to reduce gene expression variation background associated with dissimilar internode developmental status and to better focus on the consequences associated with the loss-of-function of *PanNOOT1*. The corresponding transcriptomic data have been integrated into an interactive public website (https://parasponia.plantgenie.org).

Principal component analysis (PCA) of the *P. andersonii* internode transcriptomic data highlighted a robust difference between *PanCtr-44* and the two *Pannoot1 A5* and *A10* mutants, regardless of the internode position. Indeed, two clusters formed by *PanCtr-44* samples and *Pannoot1* mutant samples diverge over the *x*-axis (PC1, 29, 43%) (Figure 6a). The PCA also revealed a divergence between *fe*lN1 versus *fe*lN2 and *fe*lN3 irrespective of the genotype, following the *y*-axis (PC2, 17, 96%) (Figure 6a). These results suggest that both *Pannoot1* mutants had similar gene expression profiles, which differed from the *PanCtr-44* control line. Furthermore, the internode age/position influenced gene expression in a genotype-independent manner.

The transcriptomic data revealed that the expression of *PanNOOT1* progressively increased in *fe*lN2 and *fe*lN3 compared to *fe*lN1; however, this increase was not statistically significant. The expression of *PanNOOT1* was drastically reduced in both *Pannoot1* mutant lines compared to the control, suggesting either that the aberrant *PanNOOT1* transcripts are degraded or that PanNOOT1 exerts a positive feedback loop on its own transcription (Figure 6e; Figure S10).

Differentially expressed transcripts (DETs) were grouped into four distinct categories of gene expression patterns (see below). Also, because transcription factors are essential regulators of plant developmental processes, including

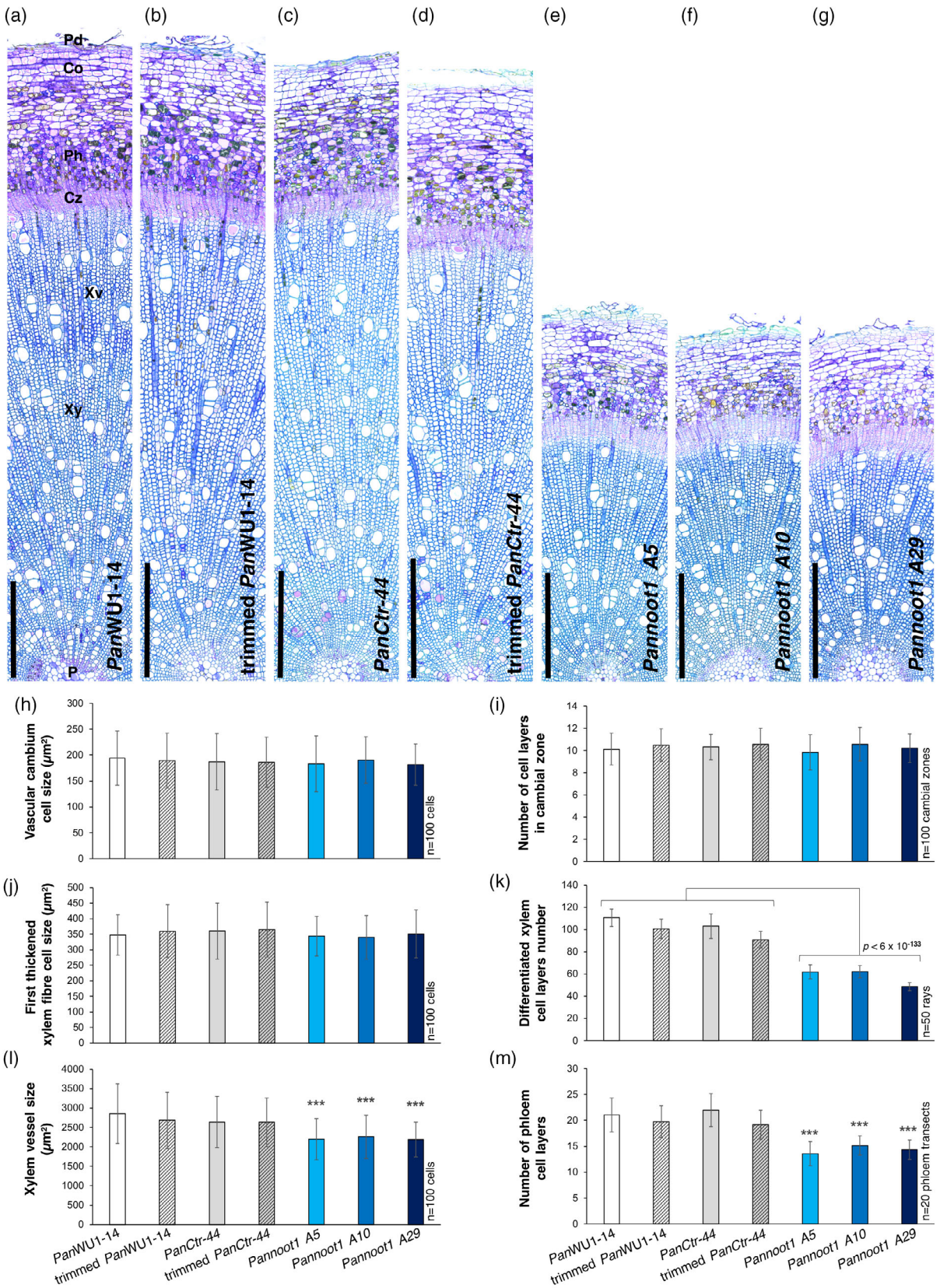

Figure 5. Histological analysis of stem tissues reveals a reduced number of xylem and phloem cell layers in *P. andersonii Pannoot1* mutants.
(a–g) Representative images of the most basal internode organizations of 10-week-old *Pan*WU1-14 (a), trimmed *Pan*WU1-14 (b), *PanCtr-44* (c), trimmed *PanCtr-44* (d), *Pannoot1 A5* (e), *Pannoot1 A10* (f) and *Pannoot1 A29* (g) genotypes. Pd, periderm; Co, cortex; Ph, phloem; Cz, cambial zone; Xv, xylem vessel; Xy, xylem fibre; P, pith. Thickness = 5 μm. Scale bars = 500 μm.
(h–m) Detailed analysis of secondary growth developmental parameters in the most basal internode of 10-week-old *Pannoot1 A5* (light blue bars), *Pannoot1 A10* (blue bars) and *Pannoot1 A29* (dark blue bars) relative to wild-type *Pan*WU1-14 (white bars), trimmed wild-type *Pan*WU1-14 (hatched white bars), transgenic control *PanCtr-44* (grey bars) and trimmed transgenic control *PanCtr-44* (hatched grey bars) plants. (h) Measurement of vascular cambium cells size. Anticlinally dividing stem cells were specifically measured.
(i) Quantification of the number of cell layers present in the cambial zone. The cells were measured along transects from anticlinally dividing vascular cambium cells until the first thickened xylem fibre cells.
(j) Measurement of the first thickened xylem fibre cells size.
(k) Quantification of the number of differentiated xylem cell layers. The cells were measured along transects from the first thickened xylem fibre cells until the pith.
(l) Measurement of xylem vessel cells size.
(m) Quantification of the number of cell layers present in the phloem. The number of phloemian cell layers were quantified along transects from anticlinally dividing stem cells until the first cortex cell layers. (h–m) The number of elements analyzed (*n*) is indicated on the right of each graph. Error bars represent SDs. Asterisks represent significant differences compared to *Pan*WU1-14 control plants (***$P < 1 \times 10^{-4}$, Student's *t*-test). For the number of differentiated xylem cell layers parameter (*k*), the statistical analysis was performed on all *Pannoot1* data and compared to all control lines ($P < 6 \times 10^{-133}$, Student's *t*-test)

secondary growth (Chao *et al.,* 2019), we explored the number of differentially expressed transcription factors in these four categories: Cat. I, genes that were significantly up-regulated in *fe*IN2 and *fe*IN3 compared to *fe*IN1, irrespective of the genotypes (437 DETs, $P < 0.01$, among which there were putative 44 transcription factors); Cat. II, genes that were significantly down-regulated in *fe*IN2 and *fe*IN3 compared to *fe*IN1, irrespective of the genotypes (391 DETs, $P < 0.01$, among which there were putative 27 transcription factors); Cat. III, genes that were significantly down-regulated in *Pannoot1* mutants compared to *PanCtr-44*, irrespective of the internode positions (3501 DETs, $P < 0.01$, among which there were putative 222 transcription factors); and Cat. IV, genes that were significantly up-regulated in *Pannoot1* mutants compared to *PanCtr-44*, irrespective of the internode positions (3677 DETs, $P < 0.01$, among which there were putative 215 transcription factors). There were no DETs that varied over both genotypes and internode positions (Figure 6b and c; Figure S11; Figure S12; Dataset S2; Dataset S3). These data indicate that the loss-of-function of *PanNOOT1* has a broad deleterious effect on transcriptional regulation in developing stem internodes.

In *A. thaliana* meristem maintenance and flowering, AtBOP1 has been shown to directly promote the expression of *ARABIDOPSIS THALIANA HOMEOBOX GENE1* (*AtATH1*) and to indirectly promote the expression of the class I *KNOX* transcription factor gene *KNOTTED-LIKE FROM ARABIDOPSIS THALIANA6* (*AtKNAT6*; Khan *et al.,* 2015). In line with this, our transcriptomic analysis revealed that the closest orthologs of *AtATH1* and *AtKNAT6* in *P. andersonii,* namely *PanATH1* and *PanKNAT6,* were significantly down-regulated in *Pannoot1* mutants (Figure 6e). These results support previous findings obtained in *A. thaliana* and suggest that PanNOOT1 might also promote the expression of *PanATH1* and *PanKNAT6* in this context of stem secondary growth.

NBCL genes, together with other meristem-to-organ-boundary genes, regulate the boundaries between SAM and lateral organs. It is possible that NBCL also plays a role in defining cambium boundaries, similarly to that in SAM. The *A. thaliana LATERAL ORGAN FUSION* (*AtLOF*) genes are involved in SAM boundary specification and regulation. Here, we found that the single ortholog of *AtLOF* genes in *P. andersonii,* named *PanLOF,* was significantly down-regulated in the *Pannoot1* mutants (Figure 6e). Together with the loss-of-function of *PanNOOT1*, the down-regulation of *PanLOF* might reflect a mis-regulation of the boundaries existing between the cambium and the adjacent xylem and phloem tissues.

Secondary cell walls of xylem fibre and vessel cells are mainly composed of lignin (20–30%), together with cellulose (40–50%) and hemicellulose (25–30%) (Pradhan Mitra and Loqué, 2014). In *A. thaliana* and *Gossypium hirsutum,* NBCL positively regulates the expression of lignin metabolism-related genes and the deposition of lignin in stems (Khan *et al.,* 2012; Zhang *et al.,* 2019). To determine whether PanNOOT1 also contributes to this process in *P. andersonii*, we investigated the expression of key lignin biosynthesis-related genes in the transcriptomic data and tested the deposition of lignin using phloroglucinol-HCl staining. In the first three fully elongated internodes (*fe*IN1, *fe*IN2 and *fe*IN3) from the shoot apex of 8-week-old plants, transcriptomic data showed that several *P. andersonii* putative homologs of the lignin metabolism-related genes were significantly down-regulated in *Pannoot1* internodes. We found that the *P. andersonii PHENYLALANINE AMMONIA-LYASE1* (*PanPAL1*), *CINNAMATE 4-HYDROXYLASE* (*PanC4H*), *4-COUMARATE COA LIGASE1* (*Pan4CL1*), *COUMARATE 3-HYDROXYLASE* (*PanC3H1*), *CAFFEOYL COENZYME A O-METHYLTRANSFERASE1* (*PanCCOAOMT1*) and *CINNAMOYL COA REDUCTASE1* (*PanCCR1*) were significantly down-regulated in *Pannoot1* mutants (Figure S13f). These results indicate that, in *Pannoot1* mutants, the lignin

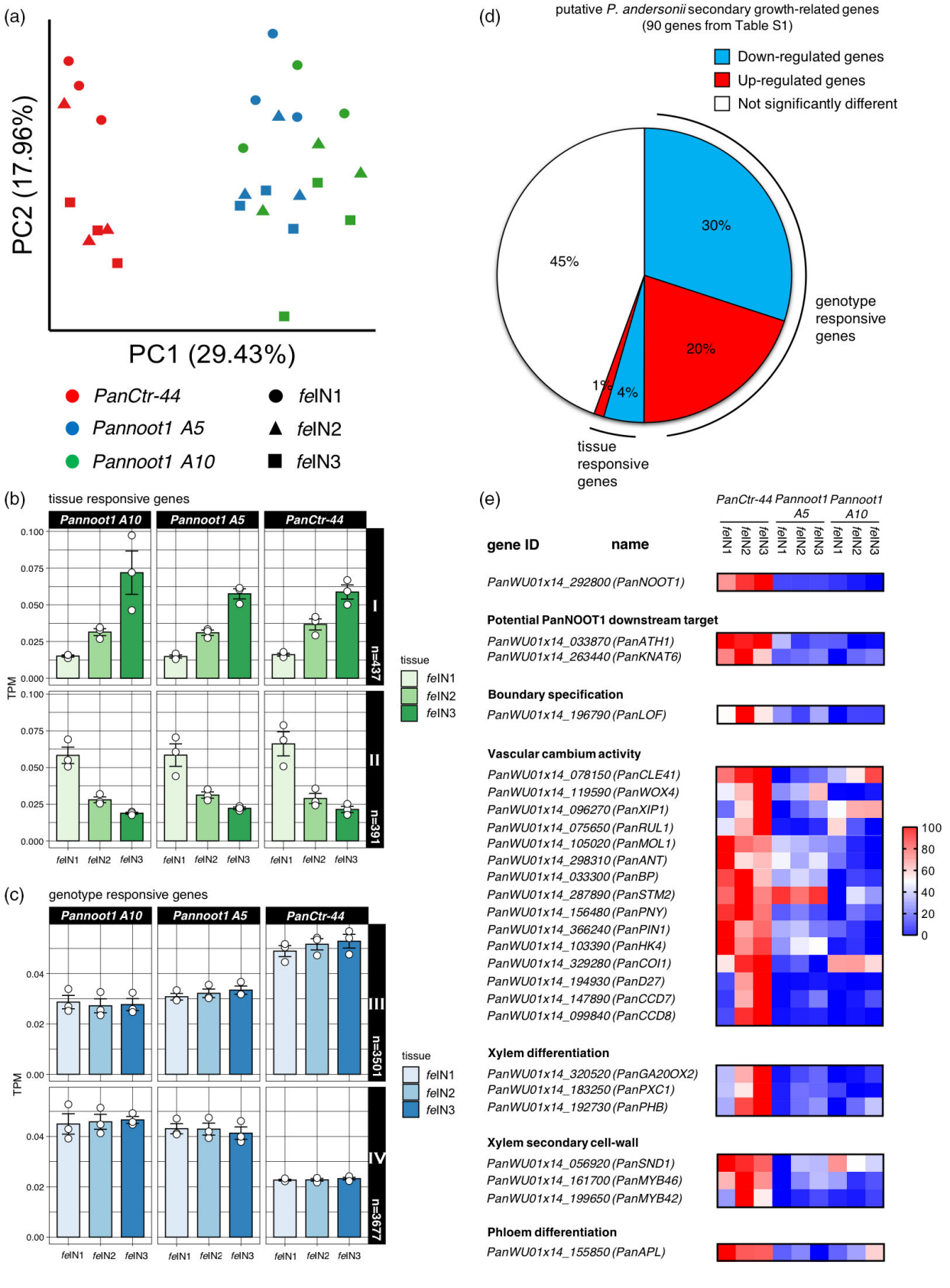

Figure 6. The *P. andersonii Pannoot1* mutants are affected in the expression of secondary growth marker genes.
(a) Principal component analysis (PCA) plot of the transcriptomic data. The PCA analysis was performed on internode samples collected from 8-week-old *PanCtr-44* (red), *Pannoot1 A5* (blue) and *Pannoot1 A10* (green). From the shoot apex, the first internode that was not shorter than the next one was defined as the first fully elongated internode *fe*lN1. Downward internodes were numbered *fe*lN2 and *fe*lN3, consecutively. The different elongated internode samples used in the analysis are indicated by distinct shapes: *fe*lN1 (circle), *fe*lN2 (triangle) and *fe*lN3 (square). All samples consisted of three biological replicates. The PCA analysis was performed on 27 transcriptomes and over 37229 *P. andersonii* genes. The first two components are shown, representing 47% of the variation in all samples.
(b,c) Differentially expressed transcripts are grouped within four distinct gene expression patterns. (b) Tissue responsive genes grouped either in tissue responsive pattern I (437 DETs, $P < 0.01$) in which genes are significantly up-regulated in older internodes compared to younger internodes, irrespective of the genotype, or in tissue responsive pattern II (391 DETs, $P < 0.01$) in which genes are significantly down-regulated in older internodes compared to younger internodes, irrespective of the genotype. (c) Genotype responsive genes can group either in the genotype responsive pattern III (3501 DETs, $P < 0.01$) in which genes are significantly down-regulated in *Pannoot1* mutants compared to *PanCtr-44*, irrespective of tissue, or in the genotype responsive pattern IV (3677 DETs, $P < 0.01$) in which genes are significantly up-regulated in *Pannoot1* mutants compared to *PanCtr-44*, irrespective of tissue. TPM, transcripts per million; *fe*lN, fully elongated internode; *n*, number of genes.
(d) A diagram showing the frequency of tissue and genotype responsive DETs among 90 *P. andersonii* genes putatively involved in secondary growth (Table S1). A detailed table showing DETs among those 90 genes is provided in Figure S14.
(e) Heatmap of significantly down-regulated transcripts related to secondary growth regulation in *Pannoot1 A5* and *A10* compared to *PanCtr-44*. *Parasponia andersonii* genes were named according to the literature for *A. thaliana* and *P. andersonii* gene accession numbers are given. Key down-regulated secondary growth-related genes were sub-divided into six groups according to their main function described in the literature: potential PanNOOT1 downstream targets, boundary specification, vascular cambium activity, xylem differentiation, xylem secondary cell wall and phloem differentiation. The heatmap scale represents normalized TPM values. For each gene, the sample with the lowest TPM value was normalized as 0 and the sample with the highest TPM value was normalized as 100. Gene abbreviations: *PanNOOT1, PanNODULE ROOT1*; *PanATH1, PanARABIDOPSIS THALIANA HOMEOBOX GENE1* (At4g32980); *PanKNAT6, PanKNOTTED-LIKE FROM ARABIDOPSIS THALIANA 6-LIKE* (At1g23380); *PanLOF, PanLATERAL ORGAN FUSION* (At1g69560, At1g26780); *PanCLE41, PanCLAVATA3/ESR-RELATED41*; *PanWOX4, PanWUSCHEL RELATED HOMEOBOX4*; *PanXIP1, PanXYLEM INTERMIXED WITH PHLOEM1*; *PanRUL1, PanREDUCED IN LATERAL GROWTH1*; *PanMOL1, PanMORE LATERAL GROWTH1*; *PanANT, PanAINTEGUMENTA*; *PanBP, PanBREVIPEDICELLUS*; *PanSTM2, PanSHOOT MERISTEMLESS2*; *PanPNY, PanPENNYWISE*; *PanPIN1, PanPINFORMED1*; *PanHK4, PanHISTIDINE KINASE4*; *PanCOI1, PanCORONATINE INSENSITIVE1*; *PanD27, PanDWARF27*; *PanCCD7, PanCAROTENOID CLEAVAGE DIOXYGENASE7*; *PanCCD8, PanCAROTENOID CLEAVAGE DIOXYGENASE8*; *PanGA20OX2, PanGIBBERELLIN 20 OXIDASE2*; *PanPXC1, PanPXY-TDR-CORRELATED1*; *PanPHB, PanPHABULOSA*; *PanSND1, PanSECONDARY WALL-ASSOCIATED NAC-DOMAIN1*; *PanMYB46, PanMYB DOMAIN PROTEIN46*; *PanMYB42, PanMYB DOMAIN PROTEIN42*; *PanAPL, PanALTERED PHLOEM DEVELOPMENT*

biosynthesis pathway is affected, even though no apparent difference in lignified cells could be observed in 16-week-old *Pannoot1* mutant plants (Figure S13a–e).

Next, we investigated the 90 *P. andersonii* genes belonging to 67 orthogroups putatively related to stem secondary growth regulation (Table S1). First, we considered whether the expression of these genes is influenced by internode position. Independently of the genotype, we found that the majority of these genes were not significantly differentially expressed in *fe*lN2 and *fe*lN3 compared to *fe*lN1. Only 1% (1/90 genes) and 4% (4/90 genes) of these genes were significantly up- or down-regulated, respectively. This is consistent with the findings obtained for the hybrid *Populus deltoides* × *Populus euramericana*, which revealed only 183 DETs when comparing two successive internodes (Chao *et al.,* 2019). Among DETs in *P. andersonii* internodes, we found that *PanSTM1* was significantly up-regulated in *fe*lN2 and *fe*lN3 compared to *fe*lN1 and that *PanTARGET OF MONOPTEROS5-LIKE1* (*PanT5L1*), *PanVND6*, *PanXYLEM CYSTEINE PEPTIDASE (PanXCP)* and *PanCONSTITUTIVE PHOTOMORPHOGENIC DWARF* (*PanCPD*) were significantly down-regulated in *fe*lN2 and *fe*lN3 compared to *fe*lN1 (Figure 6d, Figure S14). This small fraction of tissue responsive-DETs suggests that the internode samples (*fe*lN1, *fe*lN2 and *fe*lN3) were relatively homogeneous in terms of developmental status. However, in contrast to the minor effect observed for the impact of internode position on gene expression, approximately half of the putative secondary growth-related genes were significantly mis-regulated in *Pannoot1* mutants compared to *PanCtr-44*. We observed that 30% (27/90 genes) and 20% (18/90 genes) of the genes were significantly down- or up-regulated in *Pannoot1*, respectively (Figure 6d; Figure S14). Among the genes that were significantly down-regulated in *Pannoot1* compared to *PanCtr-44*, several were involved in the control of cambium activity, such as *PanCLE41*, *PanWOX4*, *PanXIP1 (PanXYLEM INTERMIXED WITH PHLOEM1)*, *PanRUL1*, *PanMOL1*, *PanANT (PanAINTEGUMENTA)*, *PanBP, PanSTM2* and *PanPNY (PanPENNYWISE)*. This suggests that PanNOOT1 positively contributes to the regulation of cambium activity genes (Figure 6e). However, we found that the expression of *PanSTM1* and *PanPXY-TDR* was not significantly different in *Pannoot1* relative to *PanCtr-44*, suggesting that the transcriptional regulation of these important cambium regulators is PanNOOT1-independent (Figure S14). In addition, we found down-regulated genes related to phytohormones, which act positively on cambium activity, notably auxin, cytokinin, jasmonic acid and strigolactone (Figure 6e). These results are in accordance with the reduced secondary growth phenotype of *Pannoot1* and also suggest that the cambium activity of *Pannoot1* mutants is impaired despite the absence of any obvious phenotype in the cambial zone itself. Besides cambium activity-related genes, other actors participating in xylem differentiation, xylem secondary cell wall deposition or phloem differentiation were found to be down-regulated in *Pannoot1* (Figure 6e). Taken together, the down-regulation of all of these important developmental markers is consistent with the reduced secondary growth phenotype observed in

Pannoot1 mutants. These results highlight the positive contribution of PanNOOT1 with respect to the promotion of cambium activity and xylogenesis.

DISCUSSION

Stem secondary growth is a key characteristic of trees. We investigated this trait in the tropical Cannabaceae tree species *P. andersonii*. Serial sectioning of the epicotyl showed the formation of the cambium at 22 days post-germination. This developmental process is associated with an increased expression of secondary growth developmental marker genes and especially cambium activity marker genes. Interestingly, the *NBCL* gene *PanNOOT1* showed a complementary expression profile relative to cambium activity marker genes suggesting antagonistic functions during cambium formation. By exploiting the transformation potential of *P. andersonii*, *PanNOOT1:GUS* reporter lines and CRISPR-Cas9 mutants were generated. We found that the expression pattern of *PanNOOT1* correlated with the secondary growth defect of the *Pannoot1* knockout mutants. Indeed, *PanNOOT1* was transcribed in the cambial zone, in phloem parenchyma, in differentiating secondary xylem cells and in differentiated secondary xylem fibres, suggesting that PanNOOT1 acts as a positive regulator of secondary growth. A similar expression pattern was also found in *P. tremula* and birch (*Betula pendula*) by high-spatial-resolution gene expression studies (Alonso-Serra *et al.,* 2019; Sundell *et al.,* 2017). In both species, the *NBCL* genes are expressed in developing phloem and in vascular cambium, as well as in developing and mature xylem tissues (Figure S15). Furthermore, we found that PanNOOT1 is required for the correct expression of secondary growth- and lignin biosynthesis-related genes. Taken together, these studies unveiled a novel function for a *NBCL* gene in stem secondary growth and demonstrated that *P. andersonii* can serve as a tree research system.

Populus species and hybrids are commonly used to explore the regulation of secondary growth in trees. The transformation efficiencies of *Populus* species are relatively low (2–16%) but are more efficient in hybrids (10–40%). Usually, transformed shoots are obtained within 1–3 months and rooted transgenic plantlets within 3–8 months depending on the genotype (Cseke *et al.,* 2007; De Block, 1990; Han *et al.,* 2000; Yevtushenko and Misra, 2010). Only recently has progress been made to transform the recalcitrant *Populus* model *P. trichocarpa* Nisqually-1. Nisqually-1 transformation efficiency now reaches 27%, transformed shoots are obtained in 1 month and obtaining rooted transgenic plantlets takes 2 months (Li *et al.,* 2017). Despite this recent advance, many transgenesis experiments are still conducted in poplar hybrids. However, CRISPR-Cas9 reverse genetics in such lines is complicated when considering the whole genome duplication that occurred in the salicoid clade (Brunner *et al.,* 2000). This duplication resulted in a large fraction of paralogous gene pairs rendering the genomes of *Populus* species and especially hybrids as relatively complex. As an example, there are approximately 8000 duplicated gene pairs in *P. trichocarpa* (Tuskan *et al.,* 2006). In many cases, paralogous genes may act redundantly, requiring the knockout or knockdown of multiple gene copies before mutant phenotypes can be observed (Bruegmann *et al.,* 2019). Therefore, the functional characterization of genes in *Populus* was often limited to over-expression analysis and/or comparative studies in *A. thaliana* (Jin *et al.,* 2017; Lu *et al.,* 2013; McCarthy *et al.,* 2010; Zhong *et al.,* 2010, 2013). By contrast, the *P. andersonii* genome organization is less complex, as we visualized by characterizing 67 orthogroups of putative secondary growth-related genes. In *P. andersonii,* these represent 90 genes, whereas in, *P. trichocarpa*, these represent 159 genes. This paralogous gene problem is also apparent for *NBCL* genes. *Populus* species have two *NBCL* paralogs, called *BLADE-ON-PETIOLE-LIKE1* and *2* (*BPL1* and *BPL2*; Magne *et al.,* 2020), whereas *P. andersonii* only possesses a single gene, namely *PanNOOT1*. Besides the reduced genome complexity of *P. andersonii,* efficient protocols for *in vitro* propagation, transformation and CRISPR-Cas9 genome editing are also available for this species (Wardhani *et al.,* 2019; van Zeijl *et al.,* 2018). Because *P. andersonii* is fast growing, self-compatible and sets seeds within approximately 5 months that can be stored for many years, this tree species is amenable for genetic dissection of tree-specific traits.

In *P. andersonii*, cambium formation and subsequent secondary growth occur within approximately 3 weeks post-germination. Here, we made a time series of sections visualizing this process in the epicotyl of a tree seedling. The transition from primary to secondary growth has also been investigated in the hybrid *P. deltoides* × *P. euramericana* but, because working with *Populus* seeds is not possible, Chao *et al*. (2019) instead used successive internodes with different stages of development. Also, the herbaceous model plant *A. thaliana* can undergo secondary growth in root, hypocotyl and stem. Cambium formation and secondary growth were investigated using this species (Fischer *et al.,* 2019; Helariutta and Bhalerao, 2003; Johnsson and Fischer, 2016; Miyashima *et al.,* 2013; Nieminen *et al.,* 2015). Time series of sections visualizing *A. thaliana* hypocotyl secondary growth were first performed by Chaffey *et al.,* 2002. Subsequently, Sankar *et al.,* 2014 provided a high-resolution atlas for *A. thaliana* hypocotyl secondary growth using two different ecotypes. In *A. thaliana* hypocotyl, the cambium formed approximately 1 week after germination; however, the flowering-induced acceleration of secondary growth only occurs after 1–2 months of growth depending on the genotype and the photoperiod conditions (Ikematsu *et al.,* 2017; Ragni *et al.,* 2011; Sibout *et al.,* 2008). Finally, *A. thaliana* secondary growth will remain

limited compared to trees. This suggests that *P. andersonii* represents a relevant model for investigating cambium formation and subsequent secondary growth.

The *P. andersonii Pannoot1* mutants have smaller xylem vessels, whereas the fibre cells are not affected. Recent studies in a *P. trichocarpa* × *P. deltoids* mapping population identified the potassium channel encoding gene *ENLARGED VESSEL ELEMENT* (*EVE*) as a regulator of xylem vessels dimension (Ribeiro *et al.,* 2020). *EVE* expression is positively controlled by SND1 and we noted that the *P. andersonii PanSND1* gene (*PanWU1x14_056920*) was down-regulated in *Pannoot1* mutant internodes (Figure 6e). We considered whether the down-regulation of *PanSND1* in *Pannoot1* mutants might affect the expression of the *P. andersonii EVE* orthologous gene, which may explain the smaller xylem vessel phenotype. However, the closest ortholog of *P. trichocarpa* EVE in *P. andersonii* (*PanWU01x14_222300*) was up-regulated in the internodes of *Pannoot1* mutants. This suggests that PanNOOT1 may function in parallel or downstream of an EVE-controlled pathway.

Research in different plant species has shown that one of the major roles of the NBCL proteins is to repress meristematic activity and promote adjacent tissues initiation and differentiation (Hepworth and Pautot, 2015; Wang *et al.,* 2016; Zadnikova and Simon, 2014). NBCL proteins are involved in the differentiation and the patterning of several organs, such as stipules, nectaries, ligule, leaves, internodes, floral meristems, flowers, abscission zones, hypocotyls, roots or nodules (Couzigou *et al.,* 2016; Couzigou *et al.,* 2012; Ha *et al.,* 2003, 2004, 2007; Hepworth *et al.,* 2005; Khan *et al.,* 2015; Khan *et al.,* 2012; Liebsch *et al.,* 2014; Magne *et al.,* 2018; McKim *et al.,* 2008; Norberg *et al.,* 2005; Tavakol *et al.,* 2015; Toriba *et al.,* 2019; Woerlen *et al.,* 2017; Yaxley *et al.,* 2001). Consistent with this role in promoting organ differentiation and patterning, in the present study, we found that PanNOOT1 promotes both xylem and phloem development in stem, and also that PanNOOT1 is required for the correct expression of key secondary growth- and lignin biosynthesis-related genes. These results are consistent with recent studies reporting that the differentiation of xylem cells is delayed in the primary root of *Medicago truncatula Mtnoot1* mutants (Shen *et al.,* 2019). However, studies in *A. thaliana* hypocotyls and roots showed that AtBOP1 and AtBOP2 repress xylem differentiation (Woerlen *et al.,* 2017). This divergence in phenotype between *A. thaliana* roots, *M. truncatula* roots and *P. andersonii* stems implies that xylem formation is possibly not a direct readout of NBCL functioning but, instead, comprises an indirect effect and depends on the (different) interacting targets. Such interacting target proteins may vary depending tissues and/or plant species. Promoter GUS reporter studies in *A. thaliana* roots and *P. andersonii* stems revealed a different spatiotemporal regulation between *AtBOP1/AtBOP2* and *PanNOOT1* in vascular tissues. In *P. andersonii* stems, *PanNOOT1* expression was detected in phloem parenchyma, in the cambial zone and in differentiating secondary xylem tissues, whereas, in *A. thaliana* roots, *AtBOP1* and *AtBOP2* were expressed in secondary phloem but not detected in the vascular cambium, nor in secondary xylem (Woerlen *et al.,* 2017). Such divergence in transcriptional regulation may contribute indirectly to the difference in phenotype in secondary xylem formation.

Studies in *A. thaliana* showed that *AtBOP1/AtBOP2* expression is repressed by homeodomain transcriptional regulators from the THREE-AMINO-ACID-LOOP-EXTENSION (TALE) family, such as the class I KNOX: BP and STM, and the BEL1-like: PENNYWISE and POUND-FOOLISH during meristem maintenance, flowering, and secondary xylem formation in roots (Khan *et al.,* 2015; Woerlen *et al.,* 2017). For example, expression of *AtBP* in root xylem represses *AtBOP1/2* expression in this tissue (Woerlen *et al.,* 2017). In agreement with such a repressing role of KNOX homeodomain transcriptional regulators, the *NBCL* gene *BPL1* is significantly down-regulated in the stem tissues of *P. tremula* × *P. alba* hybrid lines over-expressing ARK1 (orthologous to *STM*) (Liu *et al.,* 2015). Nevertheless, chromatin immunoprecipitation-sequencing analysis using ARK1 as bait did not reveal that *BPL1* or *BPL2* are direct transcriptional targets (Liu *et al.,* 2015). This suggests that, in the stem of the *P. tremula* × *P. alba* hybrid, ARK1 might repress the expression of *BPL1* by an indirect mechanism. In addition, in *P. tremula x P. alba*, over-expression of *ARK1* and *ARK2* (orthologous to *BP*) increases the size of the cambial zone and alters secondary growth. In these over-expressing mutants, the differentiation of secondary xylem tracheary elements, fibre cells and secondary phloem is inhibited. The over-expression of *ARK1* and *ARK2* is also associated with the down-regulation of secondary growth-related genes, including cell differentiation and hormonal regulation. Consistently, *ark2* mutants obtained by synthetic miRNA-suppression showed an increased secondary growth (Du *et al.,* 2009; Groover *et al.,* 2006). The phenotypes of the *ARK* over-expressor mutants are reminiscent of those found for the *P. andersonii Pannoot1* mutants because they both show an alteration of secondary growth. Taken together, these results suggest that, in tree stem secondary growth, STM/ARK1 and BP/ARK2 might act as *NBCL* repressors and that *NBCL* genes promote tree secondary growth as previously hypothesized in Khan *et al.,* 2012. Based on the results obtained in *P. andersonii* and on the data available for *A. thaliana*, *P. tremula* × *P. alba* and *G. hirsutum,* we have proposed a regulatory model for PanNOOT1 in tree secondary growth (Figure S16). In this model, PanSTM1, PanSTM2 and PanBP act as indirect repressors of *PanNOOT1*. PanNOOT1, potentially through the activation of

PanKNAT6 and *PanATH1* expression, promotes stem secondary growth and the activation of lignin metabolism-related genes.

In the present study, we have investigated to what extent *P. andersonii* could represent an alternative tree research model for untangling the genetic regulation underlying stem secondary growth. We have demonstrated the feasibility of investigating stem secondary growth using *P. andersonii* and show that this tree species represents a suitable model for applying reverse genetics. As a proof-of-concept, we knocked out and investigated the single *NBCL* gene of *P. andersonii, PanNOOT1*, and made a *nbcl* mutant in a tree species. This unveiled a novel promotive function for a *NBCL* gene in stem secondary growth.

EXPERIMENTAL PROCEDURES

Parasponia andersonii in vitro growing conditions from seeds

Mature brownish berries were collected from *P. andersonii Pan*WU1-14 trees and then the seeds were ridded of their skins by scratching. Seeds were disinfected using commercial sodium hypochlorite supplemented with a droplet of soap for 20 min and washed six times in sterile water. Seed germination was induced by continuous thermic cycles at 28°C for 4 h followed by 7°C for 4 h over 10 days. Seeds were sown on Schenk and Hildebrandt (SH) medium (pH 5.8), supplemented with 8 g L^{-1} Daishin agar. Plants were grown in a growth cabinet (Elbanton, Kerkdriel, The Netherlands) at 28°C under a 16:8 h light/dark photocycle.

Parasponia andersonii growing conditions for secondary growth assays

After *in vitro* propagation on propagation medium (SH salts, 3.2 g L^{-1}; SH vitamins, 1 g L^{-1}; sucrose, 20 g L^{-1}; BAP, 1 μg ml^{-1}; IBA, 0.1 μg ml^{-1}; MES, 3 mM, pH 5.8; Daishin agar, 8 g L^{-1}), *P. andersonii* shoots were rooted *in vitro* for 1 month on rooting medium (SH salts, 3.2 g L^{-1}; SH vitamins, 1 g L^{-1}; sucrose, 10 g L^{-1}; IBA, 1 μg ml^{-1}; NAA, 0.1 μg ml^{-1}; MES, 3 mM, pH 5.8; Daishin agar, 8 g L^{-1}). *In vitro* culture was performed in a growth cabinet (Elbanton) at 28°C under a 16:8 h light/dark photocycle and 180 μmol m^{2-1} s^{-1} light intensity. *Parasponia andersonii* plantlets were grown for 10 weeks in soil, in a greenhouse at 28°C and 85% humidity and under a 16:8 h light/dark photocycle. Plants were watered two times a week with water or nutritive solution (NH4, 1 mmol L^{-1}; K, 5.9 mmol L^{-1}; Ca; 2.7 mmol L^{-1}; Mg, 0.8 mmol L^{-1}; NO3, 9 mmol L^{-1}; SO4, 1.9 mmol L^{-1}; P, 1.1 mmol L^{-1}; Fe, 15 μmol L^{-1}; Mn, 5 μmol L^{-1}; Zn, 5 μmol L^{-1}; B, 3 μmol L^{-1}; Cu, 0.5 μmol L^{-1}; Mo, 0.5 μmol L^{-1}, pH 5.8). An additional 100 mL of NH_4NO_3 (10 mM) (pH 5.8) was provided every week to each pot to abolish eventual symbiotic associations of *P. andersonii* with bacteria naturally present in the soil. Axillary shoots suppression was performed manually, one time a week, on wild-type *Pan*WU1-14 and control plants *PanCtr-44* (van Zeijl *et al.,* 2018). Internode diameters were measured using a digital caliper (#100436; Deubba GmbH, Merzig, Germany). Secondary growth assays were performed twice.

RNA isolation from *P. andersonii* epicotyls and stems

Parasponia andersonii epicotyl or stem RNA isolation was performed as described by van Velzen *et al.,* (2017). The detailed experimental procedure for RNA isolation is provided in Methods S1.

qRT-PCR gene expression analysis

Full-length cDNAs were synthesized from 1 μg of RNA using SuperScript II Reverse Transcriptase kit (Thermo Fisher, Waltham, MA, USA) in the presence of Ribolock RNase Inhibitor (Thermo Fisher). qRT-PCR analysis was performed on 1 μl of five-fold diluted cDNA templates using iQ SYBR Green Super-mix (Bio-Rad, Hercules, CA, USA) and a CFX Connect Optical Cycler (Bio-Rad) in accordance with the manufacturer's instructions. Cycling conditions were set as: one pre-incubation cycle (95°C, 3 min) and 40 amplification cycles (denaturation, 95°C, 15 s; hybridization–elongation, 60°C, 30 s). For the melting curve, conditions were set as: (denaturation, 95°C, 10 s; hybridization, 65°C, 5 s; denaturation until 95°C with 0.5°C incrementation). Cycle thresholds and primer specificities were determined using CFX MAESTRO (Bio-Rad). *PanELONGATION FACTOR1α* (*PanEF1α*) was used as a reference gene to normalized target gene expressions (van Zeijl *et al.,* 2018). The qRT-PCR data resulted from the analysis of three biological replicates and two technical replicates. Information concerning primers used for qRT-PCR gene expression analysis is provided in Table S2.

RNA *in situ* hybridization

RNA *in situ* hybridizations were performed as described by Liu *et al.,* (2019) using the Invitrogen ViewRNA ISH Tissue1-Plex Assay kits (Thermo Fisher) and in accordance with the manufacturer's instructions. RNA *in situ* hybridization experiments were repeated three times. A detailed experimental procedure is provided in Methods S1.

Promoter:GUS:terminator reporter fusion construction

Sequence information for *PanNOOT1* (*Pan*WU01x14_292800) promoter and terminator regions were retrieved from the *P. andersonii* genome (www.parasponia.org) (van Velzen *et al.,* 2018). Promoter and terminator sequences were amplified using High Fidelity Phusion polymerase (Thermo Fisher) and cloned by golden gate cloning (Engler *et al.,* 2014). For the *PanNOOT1* promoter, three DNA fragments of 1.171, 1.401 and 0.820 kb, respectively, were cloned into level −1 pAGM1311 universal acceptors using *Bsa*I and assembled into level 0 pICH41295 acceptor (PROM + 5′UTR) using *Bpi*I. For the *PanNOOT1* terminator, a DNA fragment of 0.973 kb was cloned into level 0 pICH41276 acceptor (3′UTR + TER) using *Bpi*I. Information related to the primers used for the *promPanNOOT1:GUS:PanNOOT1ter* construction is provided in Table S3. The *PanNOOT1* promoter (3.385 kb), uidA (2.001 kb) from level 0 pICH75111 module and the *PanNOOT1* terminator (0.973 kb) were assembled into level 1 pICH47751 acceptor using *Bsa*I, resulting in a 6.359 kb construction. The construction was combined with level 1 pICH54011:dummy 1, pICH47742:*promNOS:HYGROMYCIN:NOSter* and pICH41766:level 2 end-linker 3 parts into level 2 pICSL4723 acceptor using *Bpi*I. The level 2 construction was finally introduced into *Agrobacterium tumefaciens* strain AGL1 (Lazo *et al.,* 1991) for subsequent plant transformations.

Promoter:GUS:terminator gene expression pattern

Histochemical GUS staining was performed as described in Pichon et al. (1992). Briefly, stem samples were vacuum infiltrated for 90 min (approximately 500 mmHg) in X-gluc staining buffer (50 mM phosphate buffer (pH 7.2), 1 mM potassium ferricyanide,

1 mM potassium ferrocyanide, 0.1% (w/v) SDS, 1 mM EDTA and 1.25 mM 5-bromo-4-chloro-3-indolyl-beta-d-GlcA containing cyclohexylammonium salts) and incubated at 37°C for 20 h, under darkness. Samples were fixed in 50 mM phosphate buffer (pH 7.2), 1% (v/v) glutaraldehyde and 4% (v/v) formaldehyde for 15 min under vacuum (approximately 500 mmHg). The GUS experiments were repeated two times for 7–8-week-old transgenic plants and performed on six independent transformed-lines.

Agrobacterium tumefaciens-mediated transformation of *P. andersonii*, CRISPR-Cas9 genome edition strategy and CRISPR-Cas9 mutants genotyping

These procedures were performed in accordance with the experimental procedures described by van Zeijl *et al.,* 2018 and Wardhani *et al.,* 2019. Details of the experiments are also provided in Methods S1.

Technovit sections of *P. andersonii* woody stem

Parasponia andersonii woody-stem sections were performed using Technovit 7100 (Kulzer GmbH, Wehrheim, Germany) in accordance with the manufacturer's instructions. Minor modifications were applied to the original procedure to preserve the structural integrity of the different wood tissues. As a major modification, wood samples were softened using an aqueous solution of ethylenediamine, 4%. A detailed experimental procedure is provided in Methods S1.

Phloroglucinol staining of P. andersonii stem lignins. The staining of *P. andersonii* stem lignins was performed using a phloroglucinol-HCl solution as described by Pradhan Mitra and Loqué (2014). Phloroglucinol stainings were repeated twice. A detailed experimental procedure is provided in Methods S1.

RNA-seq and data analysis. All of the internode samples used in the RNA-seq analysis consisted of three biological replicates. Single end 50-bp reads were sequenced using a BGISEQ-500 sequencing system (BGI, Shenzhen, China), yielding an average of 4.5 Gbp per sample. All reads were deposited at the European Nucleotide Archive (www.ebi.ac.uk/ena) under accession number PRJEB37036. Gene expression was quantified by pseudo-aligning the reads to the *P. andersonii* coding sequences (www.parasponia.org) (van Velzen *et al.,* 2018) using KALLISTO, version 0.43 (Bray *et al.,* 2016) with default parameters. Tissue-dependent and genotype-dependent genes were identified with the model testing framework as implemented in sleuth (Pimentel *et al.,* 2017). Briefly, for every gene, a likelihood ratio test was performed comparing a model with only an intercept term versus a model with a term for either tissue type or genotype. From this, genes with a corrected $P \leq 0.01$ were selected as varying significantly over tissue or genotype. Subsequently, distinct expression profiles were identified by performing *K*-means clustering on the significantly varying genes. Several values of *k* were tested and, for both tissue-dependent and genotype-dependent genes, no more than two visually distinct expression profiles could be identified. The code used for RNA-seq analysis is available at https://github.com/holmrenser/parasponia_code. *Parasponia andersonii* internode transcriptomic data have been integrated into an interactive website (https://parasponia.plantgenie.org) constructed using GENIE-SYS (Mannapperuma *et al.,* 2019). These transcriptomic data will be integrated into the next version of the PlantGenIE resource (Sundell *et al.,* 2015).

Parasponia andersonii transcription factor identification and analysis. *Parasponia andersonii* proteins were used as queries in BLASTP searches against *A. thaliana* protein sequences in The Arabidopsis Information Resource 10 (TAIR) (https://www.arabidopsis.org) database to obtain the closest *A. thaliana* homolog (*E*-value $\leq 1 \times 10^{-10}$). The set of *A. thaliana* transcription factors from Plant TFDB 5.0 was used as the reference database to annotate and assign *P. andersonii* transcription factors to a transcription factor family (http://planttfdb.cbi.pku.edu.cn/index.php?sp=Ath) (Jin *et al.,* 2014).

ACKNOWLEDGEMENTS

This work was supported by a NWO-VICI grant (865.13.001) to RG and by China Scholarship Council (201306040120, 201607720004, 201303250067, 201206350008) to DS, ZY, FB and YZ. We thank Arjan Van Zeijl (Wageningen University and Research, the Netherlands) for his help in the design of the *PanNOOT1* CRISPR-Cas9 RNA guides and for providing us the *PanCtr-44* CRISPR-Cas9 transgenic control. We thank Huchen Li (Beijing Agriculture University) for his help on transcriptome sequencing. We thank Dr Frédéric Lens (Leiden University, The Netherlands) for helpful discussions and advice regarding tree stem histology.

AUTHOR CONTRIBUTIONS

KM and RG conceived the project and designed the experiments. KM performed the histological kinetic of *P. andersonii* cambium establishment. DS and KM performed the qRT-PCR gene expression analysis. OK and DS performed the *PanNOOT1* RNA *in situ* hybridization. KM cloned the *promPanNOOT1:GUS* construct and performed the histological analysis. TVDM and KM genotyped the *promPanNOOT1:GUS* transgenic plants. DS generated the *Pannoot1* CRISPR-Cas9 loss-of-function mutants with the help from FB. KM and DS performed the *Pannoot1* secondary growth characterization. KM performed the wood sections of *P. andersonii* and analyzed the images. KM performed the lignin deposition analysis. DS and YZ collected the material and isolated the RNA for the transcriptomic analysis. RH performed the transcriptomic analysis and the statistical analysis. CM and NRS conceived the *P. andersonii* interactive website and integrated *P. andersonii* transcriptomic data into PopGenIE. DS, RH, ZY, OK, RG and KM analyzed the data. KM, DS, RH and ZY conceived the figures. KM, DS and RG wrote the manuscript. DS, RG and KM revised the manuscript.

CONFLICT OF INTEREST

The authors declare no conflict of interest.

DATA AVAILABILITY

All relevant data can be found within the manuscript and its supporting materials.

SUPPORTING INFORMATION

Additional Supporting Information may be found in the online version of this article.

Figure S1. Correlation between *P. andersonii* cambium establishment and shoot development.

Figure S2. *PanNOOT1* gene expression profile.

Figure S3. *PanNOOT1* promoter GUS expression pattern in *P. andersonii* stem.

Figure S4. Description of the *Pannoot1* CRISPR-Cas9 mutants.

Figure S5. Illustrations of the different genotypes used for the secondary growth assay.

Figure S6. The phellogen of *P. andersonii*.

Figure S7. *Pannoot1* A5 stems secondary growth assay at 20 weeks.

Figure S8. Stem, xylem and phloem areas are reduced in *Pannoot1*.

Figure S9. *Parasponia andersonii* internode sections corresponding to the samples used in the transcriptomic analysis.

Figure S10. *Parasponia andersonii PanNOOT1* RNA-seq expression profile in *PanCtr-44* and *Pannoot1 A5* and *A10* internodes.

Figure S11. Top ten enriched Gene Ontology terms.

Figure S12. Tissue- and genotype-dependent differentially expressed transcription factors.

Figure S13. Lignin deposition and heatmap of putative lignin biosynthesis-related genes expression in *Pannoot1* internodes.

Figure S14. Tissue- and genotype-dependent expression of key secondary growth-related genes.

Figure S15. Gene expression profiles of *Populus tremula* and *Betula pendula* BOP genes in stem tissues.

Figure S16. A model for *PanNOOT1* stem secondary growth regulation.

Table S1. Secondary growth-related orthogroups. Orthogroup numbering according to van Velzen et al. (2018).

Table S2. Primers used for qRT-PCR.

Table S3. Primers used for *promPanNOOT1:GUS:PanNOOT1ter* golden gate cloning.

Dataset S1. Phylogenetic reconstruction analysis of putative *P. andersonii* secondary growth-related genes orthologs.

Dataset S2. Lists of the genotype- and tissue-dependent differentially expressed transcripts and transcripts per million values.

Dataset S3. Lists of differentially expressed transcription factors.

Methods S1. Enhanced experimental procedures.

REFERENCES

Agusti, J., Lichtenberger, R., Schwarz, M., Nehlin, L. & Greb, T. (2011) Characterization of transcriptome remodeling during cambium formation identifies MOL1 and RUL1 as opposing regulators of secondary growth. *PLoS Genetics*, **7**, e1001312.

Aida, M. & Tasaka, M. (2006a) Genetic control of shoot organ boundaries. *Current Opinion in Plant Biology*, **9**, 72–77. https://doi.org/10.1016/j.pbi.2005.11.011.

Aida, M. & Tasaka, M. (2006b) Morphogenesis and patterning at the organ boundaries in the higher plant shoot apex. *Plant Molecular Biology*, **60**, 915–928. https://doi.org/10.1007/s11103-005-2760-7.

Alonso-Serra, J., Safronov, O., Lim, K.J., Fraser-Miller, S.J., Blokhina, O.B., Campilho, A. *et al.* (2019) Tissue-specific study across the stem reveals the chemistry and transcriptome dynamics of birch bark. *New Phytologist*, **222**(4), 1816–1831. https://doi.org/10.1111/nph.15725.

Barnett, J.R. (1981) Secondary xylem cell development. In: Barnett, J.R. (Ed.) *Xylem cell development*. London: Castle House, pp. 47–95.

Barton, M.K. (2010) Twenty years on: The inner workings of the shoot apical meristem, a developmental dynamo. *Developmental Biology*, **341**, 95–113.

Becking, J.H. (1992) The Rhizobium symbiosis of the non-legume Parasponia. In Stacey, G.S., Evans, H.J. & Burris, R.H., eds. *Biological nitrogen fixation*. New York, NY: Routledge, pp. 497–559.

Behm, J.E., Geurts, R. & Kiers, E.T. (2014) Parasponia: A novel system for studying mutualism stability. *Trends in Plant Science*, **19**, 757–763. https://doi.org/10.1016/j.tplants.2014.08.007.

Bonke, M., Thitamadee, S., Mahonen, A.P., Hauser, M.T. & Helariutta, Y. (2003) APL regulates vascular tissue identity in Arabidopsis. *Nature*, **426**, 181–186.

Brackmann, K. & Greb, T. (2014) Long- and short-distance signaling in the regulation of lateral plant growth. *Physiologia Plantarum*, **151**, 134–141.

Bray, N.L., Pimentel, H., Melsted, P. & Pachter, L. (2016) Near-optimal probabilistic RNA-seq quantification. *Nature Biotechnology*, **34**(5), 525–527.

Bruegmann, T., Deecke, K. & Fladung, M. (2019) Evaluating the efficiency of gRNAs in CRISPR/Cas9 mediated genome editing in Poplars. *International Journal of Molecular Sciences*, **20**, 3623. https://doi.org/10.3390/ijms20153623.

Brunner, A.M., Rottmann, W.H., Sheppard, L.A., Krutovskii, K., Di Fazio, S.P., Leonardi, S. *et al.* (2000) Structure and expression of duplicate AGAMOUS orthologs in poplar. *Plant Molecular Biology*, **44**, 619–634.

Bu, F., Rutten, L., Roswanjaya, Y.P., Kulikova, O., Rodriguez-Franco, M., Ott, T. *et al.* (2020) Mutant analysis in the nonlegume *Parasponia andersonii* identifies NIN and NF-YA1 transcription factors as a core genetic network in nitrogen-fixing nodule symbioses. *New Phytologist*, **226**, 541–554. https://doi.org/10.1111/nph.16386.

Campbell, L. & Turner, S. (2017) Regulation of vascular cell division. *Journal of Experimental Botany*, **68**(1), 27–43. https://doi.org/10.1093/jxb/erw448.

Carlsbecker, A., Lee, J.Y., Roberts, C.J., Dettmer, J., Lehesranta, S., Zhou, J. *et al.* (2010) Cell signalling by microRNA165/6 directs gene dose-dependent root cell fate. *Nature*, **465**, 316–321.

Chaffey, N., Cholewa, E., Regan, S. & Sundberg, B. (2002) Secondary xylem development in Arabidopsis: A model for wood formation. *Physiologia Plantarum*, **114**(4), 594–600. https://doi.org/10.1034/j.1399-3054.2002.1140413.x.

Chao, Q., Gao, Z.F., Zhang, D., Zhao, B.G., Dong, F.Q., Fu, C.X. *et al.* (2019) The developmental dynamics of the Populus stem transcriptome. *Plant Biotechnology Journal*, https://doi.org/10.1111/pbi.12958.

Couzigou, J.M., Magne, K., Mondy, S., Cosson, V., Clements, J. & Ratet, P. (2016) The legume NOOT-BOP-COCH-LIKE genes are conserved regulators of abscission, a major agronomical trait in cultivated crops. *New Phytologist*, **209**, 228–240. https://doi.org/10.1111/nph.13634.

Couzigou, J.M., Zhukov, V., Mondy, S., Abu el Heba, G., Cosson, V., Ellis, T.H. *et al.* (2012) NODULE ROOT and COCHLEATA maintain nodule development and are legume orthologs of Arabidopsis BLADE-ON-PETIOLE genes. *The Plant Cell*, **24**, 4498–4510. https://doi.org/10.1105/tpc.112.103747.

Cseke, L.J., Cseke, S.B. & Podila, G.K. (2007) High efficiency poplar transformation. *Plant Cell Reports*, **26**(9), 1529–1538. https://doi.org/10.1007/s00299-007-0365-0.

De Block, M. (1990) Factors influencing the tissue culture and the *Agrobacterium tumefaciens*-mediated transformation of hybrid aspen and poplar clones. *Plant Physiology*, **93**, 1110–1116. https://doi.org/10.1104/pp.93.3.1110.

Dong, Z.B., Li, W., Unger-Wallace, E., Yang, J., Vollbrecht, E. & Chuck, G. (2017) Ideal crop plant architecture is mediated by tassels replace upper ears1, a BTB/POZ ankyrin repeat gene directly targeted by TEOSINTE BRANCHED1. *Proceedings of the National Academy of Sciences of the United States of America*, **114**, E8656–E8664. https://doi.org/10.1073/pnas.1714960114.

Du, J., Mansfield, S.D. & Groover, A.T. (2009) The Populus homeobox gene ARBORKNOX2 regulates cell differentiation during secondary growth. *Plant Journal*, **60**, 1000–1014.

Du, J., Miura, E., Robischon, M., Martinez, C. & Groover, A. (2011) The Populus Class III HD-ZIP transcription factor POPCORONA affects cell differentiation during secondary growth of woody stems. *PLoS One*, **6**, e17458.

Emms, D.M. & Kelly, S. (2015) OrthoFinder: Solving fundamental biases in whole genome comparisons dramatically improves orthogroup inference accuracy. *Genome Biology*, **16**, 157.

Engler, C., Youles, M., Gruetzner, R., Ehnert, T.M., Werner, S., Jones, J.D.G. *et al.* (2014) A golden gate modular cloning toolbox for plants. ACS. *Synthetic Biology*, **3**, 839–843. https://doi.org/10.1021/sb4001504.

Etchells, J.P., Mishra, L.S., Kumar, M., Campbell, L. & Turner, S.R. (2015) Wood formation in trees is increased by manipulating PXY-regulated cell division. *Current Biology*, **25**, P1050–P1055.

Etchells, J.P., Provost, C.M., Mishra, L. & Turner, S.R. (2013) WOX4 and WOX14 act downstream of the PXY receptor kinase to regulate plant vascular proliferation independently of any role in vascular organisation. *Development*, **140**, 2224–2234.

Etchells, J.P. & Turner, S.R. (2010) The PXY-CLE41 receptor ligand pair defines a multifunctional pathway that controls the rate and orientation of vascular cell division. *Development*, **137**, 767–774.

Evert, R.F. & Eichhorn, S.E. (2006) *Esau's plant anatomy*. Hoboken, NJ: Wiley & Sons.

Fischer, U., Kucukoglu, M., Helariutta, Y. & Bhalerao, R.P. (2019) The dynamics of cambial stem cell activity. *Annual Review of Plant Biology*, **70**, 293–319. https://doi.org/10.1146/annurev-arplant-050718-100402.

Fisher, K. & Turner, S. (2007) PXY, a receptor-like kinase essential for maintaining polarity during plant vascular-tissue development. *Current Biology*, **17**, 1061–1066.

Groover, A., Mansfield, S., DiFazio, S., Dupper, G., Fontana, J., Millar, R. *et al.* (2006) The Populus homeobox gene ARBORKNOX1 reveals overlapping mechanisms regulating the shoot apical meristem and the vascular cambium. *Plant Molecular Biology*, **61**, 917–932.

Gursanscky, N.R., Jouannet, V., Grunwald, K., Sanchez, P., Laaber-Schwarz, M. & Greb, T. (2016) MOL1 is required for cambium homeostasis in Arabidopsis. *The Plant Journal*, **86**, 210–220.

Ha, C.M., Jun, J.H., Nam, H.G. & Fletcher, J.C. (2004) BLADE-ON-PETIOLE1 encodes a BTB/POZ domain protein required for leaf morphogenesis in *Arabidopsis thaliana*. *Plant and Cell Physiology*, **45**(10), 1361–1370. https://doi.org/10.1093/pcp/pch201.

Ha, C.M., Jun, J.H., Nam, H.G. & Fletcher, J.C. (2007) BLADE-ON-PETIOLE1 and 2 control Arabidopsis lateral organ fate through regulation of LOB domain and adaxial-abaxial polarity genes. *The Plant Cell*, **19**, 1809–1825. https://doi.org/10.1105/tpc.107.051938.

Ha, C.M., Kim, G.T., Kim, B.C., Jun, J.H., Soh, M.S., Ueno, Y. *et al.* (2003) The BLADE-ON-PETIOLE 1 gene controls leaf pattern formation through the modulation of meristematic activity in Arabidopsis. *Development*, **130**, 161–172.

Han, K.H., Meilan, R., Ma, C. & Strauss, S.H. (2000) An Agrobacterium tumefaciens transformation protocol effective on a variety of cottonwood hybrids (genus *Populus*). *Plant Cell Reports*, **19**, 315–320.

Helariutta, Y. & Bhalerao, R. (2003) Between Xylem and Phloem: The genetic control of cambial activity in plants. *Plant Biology*, **5**, 465–472. https://doi.org/10.1055/s-2003-44780.

Hepworth, S.R. & Pautot, V.A. (2015) Beyond the divide: Boundaries for patterning and stem cell regulation in plants. *Frontiers in Plant Science*, **6**, 1052. https://doi.org/10.3389/fpls.2015.01052.

Hepworth, S.R., Zhang, Y., McKim, S., Li, X. & Haughn, G.W. (2005) BLADE-ON-PETIOLE–dependent signaling controls leaf and floral patterning in Arabidopsis. *The Plant Cell*, **17**, 1434–1448. https://doi.org/10.1105/tpc.104.030536

Hirakawa, Y., Kondo, Y. & Fukuda, H. (2010) TDIF peptide signaling regulates vascular stem cell proliferation via the WOX4 homeobox gene in Arabidopsis. *Plant Cell Online*, **22**, 2618–2629.

Hirakawa, Y., Shinohara, H., Kondo, Y., Inoue, A., Nakanomyo, I., Ogawa, M. *et al.* (2008) Non-cell-autonomous control of vascular stem cell fate by a CLE peptide/receptor system. *Proceedings of the National Academy of Sciences of the United States of America*, **105**(39), 15208–15213. https://doi.org/10.1073/pnas.0808444105.

Holmer, R., van Velzen, R., Geurts, R., Bisseling, T., de Ridder, D. & Smit, S. (2019) GeneNoteBook, a collaborative notebook for comparative genomics. *Bioinformatics*, **35**(22), 4779–4781. https://doi.org/10.1093/bioinformatics/btz491.

Ikematsu, S., Tasaka, M., Torii, K.U. & Uchida, N. (2017) ERECTA-family receptor kinase genes redundantly prevent premature progression of secondary growth in the Arabidopsis hypocotyl. *New Phytologist*, **213**, 1697–1709. https://doi.org/10.1111/nph.14335.

Ilegems, M., Douet, V., Meylan-Bettex, M., Uyttewaal, M., Brand, L., Bowman, J.L. *et al.* (2010) Interplay of auxin, KANADI and Class III HD-ZIP transcription factors in vascular tissue formation. *Development*, **137**, 975–984.

Immanen, J., Nieminen, K., Smolander, O.P., Kojima, M., Alonso Serra, J., Koskinen, P. *et al.* (2016) Cytokinin and auxin display distinct but interconnected distribution and signaling profiles to stimulate cambial activity. *Current Biology*, **26**, 1990–1997.

Ishaq, R.M., Hairiah, K., Alfian, I. & van Noordwijk, M. (2020) Natural regeneration after volcanic eruptions: Resilience of the non-legume nitrogen-fixing tree *Parasponia rigida*. *Frontiers in Forests and Global Change*, **3**, 562303. https://doi.org/10.3389/ffgc.2020.562303.

Ito, Y., Nakanomyo, I., Motose, H., Iwamoto, K., Sawa, S., Dohmae, N. *et al.* (2006) Dodeca-CLE peptides as suppressors of plant stem cell differentiation. *Science*, **313**, 842–845.

Jahan, M.S., Chowdhury, N. & Ni, Y. (2010) Effect of different locations on the morphological, chemical, pulping and papermaking properties of *Trema orientalis* (Nalita). *Bioresource Technology*, **101**, 1892–1898.

Jahan, M.S. & Mun, S.P. (2003) Characterization of Nalita wood (*Trema orientalis*) as a source of fiber for papermaking. (Part I): Anatomical, morphological and chemical properties. *Journal of Korea Technical Association of The Pulp and Paper Industry*, **35**, 72–79.

Jahan, M.S., Rubaiyat, A. & Sabina, R. (2007) Evaluation of cooking processes for *Trema orientalis* pulping. *Journal of Scientific & Industrial Research*, **66**, 853–859.

Ji, J., Strable, J., Shimizu, R., Koenig, D., Sinha, N. & Scanlon, M.J. (2010) WOX4 promotes procambial development. *Plant Physiology*, **152**, 1346–1356.

Jin, J., Zhang, H., Kong, L., Gao, G. & Luo, J. (2014) PlantTFDB 3.0: A portal for the functional and evolutionary study of plant transcription factors. *Nucleic Acids Research*, **42**, D1182–D1187.

Jin, Y.L., Tang, R.J., Wang, H.H., Jiang, C.M., Bao, Y., Yang, Y. *et al.* (2017) Overexpression of *Populus trichocarpa* CYP85A3 promotes growth and biomass production in transgenic trees. *Plant Biotechnology Journal*, **15**, 1309–1321. https://doi.org/10.1111/pbi.12717.

Johnsson, C. & Fischer, U. (2016) Cambial stem cells and their niche. *Plant Science*, **252**, 239–245.

Jost, M., Taketa, S., Mascher, M., Himmelbach, A., You, T., Shahinnia, F. *et al.* (2016) A homolog of BLADE-ON-PETIOLE 1 and 2 (BOP1/2) controls internode length and homeotic changes of the barley inflorescence. *Plant Physiology*, **171**(2), 1113–1127. https://doi.org/10.1104/pp.16.00124.

Jun, J.H., Ha, C.M. & Fletcher, J.C. (2010) BLADE-ON-PETIOLE1 coordinates organ determinacy and axial polarity in Arabidopsis by directly activating ASYMMETRIC LEAVES2. *The Plant Cell*, **22**, 62–76.

Khan, M., Ragni, L., Tabb, P., Salasini, B.C., Chatfield, S., Datla, R. *et al.* (2015) Repression of lateral organ boundary genes by PENNYWISE and POUND-FOOLISH is essential for meristem maintenance and flowering in *Arabidopsis thaliana*. *Plant Physiology*, **169**(3), 2166–2186. https://doi.org/10.1104/pp.15.00915.

Khan, M., Xu, H. & Hepworth, S.R. (2014) BLADE-ON-PETIOLE genes: Setting boundaries in development and defense. *Plant Science*, **215–216**, 157–171. https://doi.org/10.1016/j.plantsci.2013.10.019.

Khan, M., Xu, M., Murmu, J., Tabb, P., Liu, Y., Storey, K. *et al.* (2012) Antagonistic interaction of BLADE-ON-PETIOLE1 and 2 with BREVIPEDICELLUS and PENNYWISE regulates Arabidopsis inflorescence architecture. *Plant Physiology*, **158**, 946–960. https://doi.org/10.1104/pp.111.188573.

Kubo, M., Udagawa, M., Nishikubo, N., Horiguchi, G., Yamaguchi, M., Ito, J. *et al.* (2005) Transcription switches for protoxylem and metaxylem vessel formation. *Genes & Development*, **19**, 1855–1860.

Kucukoglu, M., Nilsson, J., Zheng, B., Chaabouni, S. & Nilsson, O. (2017) WUSCHEL-RELATED HOMEOBOX4 (WOX4)-like genes regulate cambial cell division activity and secondary growth in Populus trees. *New Phytologist*, **215**, 642–657.

Larson, P.R. (1994) *The vascular cambium: Development and structure*. Berlin: Springer-Verlag.

Lazo, G.R., Stein, P.A. & Ludwig, R.A. (1991) A DNA transformation-competent Arabidopsis genomic library in Agrobacterium. *Biotechnology*, **9**, 963–967. https://doi.org/10.1038/nbt1091-963.

Li, S., Zhen, C., Xu, W., Wang, C. & Cheng, Y. (2017) Simple, rapid and efficient transformation of genotype Nisqually-1: A basic tool for the first sequenced model tree. *Scientific Reports*, **7**, 2638. https://doi.org/10.1038/s41598-017-02651-x.

Liebsch, D., Sunaryo, W., Holmlund, M., Norberg, M., Zhang, J., Hall, H.C. *et al.* (2014) Class I KNOX transcription factors promote differentiation of cambial derivatives into xylem fibers in the Arabidopsis hypocotyl. *Development*, **141**(22), 4311–4319.

Little, C.A., MacDonald, J.E. & Olsson, O. (2002) Involvement of Indole-3-acetic acid in fascicular and interfascicular cambial growth and

interfascicular extraxylary fiber differentiation in *Arabidopsis thaliana* inflorescence stems. *International Journal of Plant Sciences*, **163**, 519–529.

Liu, J., Rutten, L., Limpens, E., van der Molen, T., van Velzen, R., Chen, R. *et al.* (2019) A remote cis-regulatory region is required for NIN expression in the pericycle to initiate nodule primordium formation in *Medicago truncatula*. *The Plant Cell*, **31**, 68–83. https://doi.org/10.1105/tpc.18.00478.

Liu, L., Ramsay, T., Zinkgraf, M., Sundell, D., Street, N.R., Filkov, V. *et al.* (2015) A resource for characterizing genome-wide binding and putative target genes of transcription factors expressed during secondary growth and wood formation in Populus. *The Plant Journal*, **82**(5), 887–898. https://doi.org/10.1111/tpj.12850.

Liu, Z., Yang, N., Lv, Y., Pan, L., Lv, S., Han, H. & *et al.* (2016) The CLE gene family in *Populus trichocarpa*. *Plant Signal Behaviour*, **11**, e1191734.

Lu, S., Li, Q., Wei, H., Chang, M.J., Tunlaya-Anukit, S., Kim, H. *et al.* (2013) Ptr-miR397a is a negative regulator of laccase genes affecting lignin content in *Populus trichocarpa*. *PNAS*, **110**(26), 10848–10853. https://doi.org/10.1073/pnas.1308936110.

Magne, K., George, J., Berbel Tornero, A., Broquet, B., Madueño, F., Andersen, S.U. *et al.* (2018) *Lotus japonicus* NOOT-BOP-COCH-LIKE1 is essential for nodule, nectary, leaf and flower development. *The Plant Journal*, **94**, 880–894. https://doi.org/10.1111/tpj.13905.

Magne, K., Liu, S., Massot, S., Dalmais, M., Morin, H., Sibout, R. *et al.* (2020) Roles of BdUNICULME4 and BdLAXATUM-A in the non-domesticated grass Brachypodium distachyon. *The Plant Journal*, **103**(2), 645–659.

Mannapperuma, C., Waterworth, J. & Street, N.R. (2019) GenIE-Sys: Genome integrative explorer system. BioRxiv, https://doi.org/10.1101/808881.

Mazur, E., Kurczynska, E.U. & Friml, J. (2014) Cellular events during interfascicular cambium ontogenesis in inflorescence stems of Arabidopsis. *Protoplasma*, **251**, 1125–1139.

McCarthy, R.L., Zhong, R., Fowler, S., Lyskowski, D., Piyasena, H., Carleton, K. *et al.* (2010) The Poplar MYB transcription factors, PtrMYB3 and PtrMYB20, are involved in the regulation of secondary wall biosynthesis. *Plant and Cell Physiology*, **51**(6), 1084–1090. https://doi.org/10.1093/pcp/pcq064.

McKim, S.M., Stenvik, G.E., Butenko, M.A., Kristiansen, W., Cho, S.K., Hepworth, S.R. *et al.* (2008) The BLADE-ON-PETIOLE genes are essential for abscission zone formation in Arabidopsis. *Development*, **135**, 1537–1546. https://doi.org/10.1242/dev.012807.

Mellerowicz, E.J., Baucher, M., Sundberg, B. & Boerjan, W. (2001) Unravelling cell wall formation in the woody dicot stem. *Plant Molecular Biology*, **47**, 239–274.

Mitsuda, N., Iwase, A., Yamamoto, H., Yoshida, M., Seki, M., Shinozaki, K. *et al.* (2007) NAC transcription factors, NST1 and NST3, are key regulators of the formation of secondary walls in woody tissues of Arabidopsis. *The Plant Cell*, **19**, 270–280.

Miyashima, S., Sebastian, J., Lee, J.Y. & Helariutta, Y. (2013) Stem cell function during plant vascular development. *The EMBO Journal*, **32**, 178–193. https://doi.org/10.1038/emboj.2012.301.

Nieminen, K., Blomster, T., Helariutta, Y. & Mahonen, A.P. (2015) Vascular cambium development. *The Arabidopsis Book*, **13**, e0177. https://doi.org/10.1199/tab.0177.

Nilsson, J., Karlberg, A., Antti, H., Lopez-Vernaza, M., Mellerowicz, E., Perrot-Rechenmann, C. *et al.* (2008) Dissecting the molecular basis of the regulation of wood formation by auxin in hybrid aspen. *The Plant Cell*, **20**, 843–855.

Norberg, M., Holmlund, M. & Nilsson, O. (2005) The BLADE ON PETIOLE genes act redundantly to control the growth and development of lateral organs. *Development*, **132**, 2203–2213. https://doi.org/10.1242/dev.01815.

Ohashi-Ito, K., Oda, Y. & Fukuda, H. (2010) Arabidopsis VASCULAR-RELATED NAC-DOMAIN6 directly regulates the genes that govern programmed cell death and secondary wall formation during xylem differentiation. *The Plant Cell*, **22**, 3461–3473.

Op den Camp, R., Streng, A., De Mita, S., Cao, Q., Polone, E., Liu, W. *et al.* (2011) LysM-type mycorrhizal receptor recruited for rhizobium symbiosis in non-legume Parasponia. *Science*, **331**, 909–912.

Pichon, M., Journet, E., Dedieu, A., De Billy, F., Truchet, G. & Barker, D.G. (1992) Rhizobium meliloti elicits transient expression of the early nodulin gene ENOD12 in the differentiating root epidermis of transgenic alfalfa. *The Plant Cell*, **4**, 1199–1211.

Pimentel, H.J., Bray, N., Puente, S., Melsted, P. & Pachter, L. (2017) Differential analysis of RNA-Seq incorporating quantification uncertainty. *Nature Methods*, **14**(7), 687–690. https://doi.org/10.1038/nmeth.4324.

Pradhan Mitra, P. & Loqué, D. (2014) Histochemical staining of *Arabidopsis thaliana* secondary cell wall elements. *Journal of Visualized Experiments*, **87**, e51381. https://doi.org/10.3791/51381.

Prigge, M.J., Otsuga, D., Alonso, J.M., Ecker, J.R., Drews, G.N. & Clark, S.E. (2005) Class III homeodomain-leucine zipper gene family members have overlapping, antagonistic, and distinct roles in Arabidopsis development. *The Plant Cell*, **17**, 61–76.

Ragni, L. & Greb, T. (2018) Secondary growth as a determinant of plant shape and form. *Seminars in Cell & Developmental Biology*, **79**, 58–67. https://doi.org/10.1016/j.semcdb.2017.08.050.

Ragni, L., Nieminen, K., Pacheco-Villalobos, D., Sibout, R., Schwechheimer, C. & Hardtke, C.S. (2011) Mobile gibberellin directly stimulates Arabidopsis hypocotyl xylem expansion. *The Plant Cell*, **23**(4), 1322–1336.

Ribeiro, C.L., Conde, D., Balmant, K.M., Dervinis, C., Johnson, M.G., McGrath, A.P. *et al.* (2020) The uncharacterized gene EVE contributes to vessel element dimensions in *Populus*. *Proceedings of the National Academy of Sciences of the United States of America*, **117**(9), 5059–5066. https://doi.org/10.1073/pnas.1912434117.

Rutten, L., Miyata, K., Roswanjaya, Y.P., Huisman, R., Bu, F., Hartog, M. *et al.* (2020) Duplication of symbiotic lysin motif receptors predates the evolution of nitrogen-fixing nodule symbiosis. *Plant Physiology*, **184**(2), 1004–1023. https://doi.org/10.1104/pp.19.01420.

Sankar, M., Nieminen, K., Ragni, L., Xenarios, I. & Hardtke, C.S. (2014) Automated quantitative histology reveals vascular morphodynamics during Arabidopsis hypocotyl secondary growth. *Elife*, **3**, e01567. https://doi.org/10.7554/eLife.01567.

Schrader, J., Nilsson, J., Mellerowicz, E., Berglund, A., Nilsson, P., Hertzberg, M. *et al.* (2004) A high-resolution transcript profile across the wood-forming meristem of poplar identifies potential regulators of cambial stem cell identity. *The Plant Cell*, **16**, 2278–2292.

Shen, D., Kulikova, O., Guhl, K., Franssen, H., Kohlen, W., Bisseling, T. *et al.* (2019) *MtNOOT1* is required for coordinated apical-basal development of the root. *BMC Plant Biology*, **19**, 571. https://doi.org/10.1186/s12870-019-2194-z.

Shen, D., Magne, K., Kulikova, O., Bu, F., Zhang, Y., Wang, J. *et al.* (unpublished data). PanNODULE ROOT1 is a BLADE-ON-PETIOLE gene that regulates branching, stipule formation and leaf patterning in the tropical Cannabaceae tree Parasponia andersonii.

Shen, D., Xiao, T.T., van Velzen, R., Kulikova, O., Gong, X., Geurts, R. *et al.* (2020) A homeotic mutation changes legume nodule ontogeny into actinorhizal-type ontogeny. *The Plant Cell*, **32**(6), 1868–1885. https://doi.org/10.1105/tpc.19.00739.

Sibout, R., Plantegenet, S. & Hardtke, C.S. (2008) Flowering as a condition for xylem expansion in Arabidopsis hypocotyl and root. *Current Biology*, **18**, 458–463. https://doi.org/10.1016/j.cub.2008.02.070.

Suer, S., Agusti, J., Sanchez, P., Schwarz, M. & Greb, T. (2011) WOX4 imparts auxin responsiveness to cambium cells in Arabidopsis. *The Plant Cell*, **23**, 3247–3259.

Sundell, D., Mannapperuma, C., Netotea, S., Delhomme, N., Lin, Y.C., Sjödin, A. *et al.* (2015) The plant genome integrative explorer resource: PlantGenIE.org. *New Phytologist*, **208**(4), 1149–1156. https://doi.org/10.1111/nph.13557.

Sundell, D., Street, N.R., Kumar, M., Mellerowicz, E.J., Kucukoglu, M., Johnsson, C. *et al.* (2017) AspWood: High-spatial-resolution transcriptome profiles reveal uncharacterized modularity of wood formation in *Populus tremula*. *The Plant Cell*, **29**, 1585–1604. https://doi.org/10.1105/tpc.17.00153.

Tavakol, E., Okagaki, R., Verderio, G., Shariati, J.V., Hussien, A., Bilgic, H. *et al.* (2015) The barley UNICULME4 gene encodes a BLADE-ON-PETIOLE-like protein that controls tillering and leaf patterning. *Plant Physiology*, **168**(1), 164–174. https://doi.org/10.1104/pp.114.252882.

Toriba, T., Tokunaga, H., Shiga, T., Nie, F., Naramoto, S., Honda, E. *et al.* (2019) BLADE-ON-PETIOLE genes temporally and developmentally regulate the sheath to blade ratio of rice leaves. *Nature communications*, **10**, 619. https://doi.org/10.1038/s41467-019-08479-5.

Trinick, M.J. (1980) Growth of Parasponia in agar tube culture and symbiotic effectiveness of isolates from Parasponia spp. *New Phytologist*, **85**, 37–45. https://doi.org/10.1111/j.1469-8137.1980.tb04446.x.

Tuominen, H., Puech, L., Fink, S. & Sundberg, B. (1997) A radial concentration gradient of indole-3-acetic acid is related to secondary xylem development in hybrid aspen. *Plant Physiology*, **115**, 577–585.

Tuskan, G.A., Difazio, S., Jansson, S., Bohlmann, J., Grigoriev, I., Hellsten, U. *et al.* (2006) The genome of black cottonwood, *Populus trichocarpa* (Torr. & Gray). *Science*, **313**, 1596–1604.

van Velzen, R., Holmer, R., Bu, F., Rutten, L., van Zeijl, A., Liu, W. *et al.* (2017) Parallel loss of symbiosis genes in relatives of nitrogen-fixing non-legume Parasponia. bioRxiv 169706. https://doi.org/10.1101/169706.

van Velzen, R., Holmer, R., Bu, F., Rutten, L., van Zeijl, A., Liu, W. *et al.* (2018) Comparative genomics of the non-legume Parasponia reveals insights into evolution of nitrogen-fixing rhizobium symbioses. *Proceedings of the National Academy of Sciences of the United States of America*, **115**(20), E4700–E4709. https://doi.org/10.1073/pnas.1721395115.

van Zeijl, A., Wardhani, T.A.K., Seifi Kalhor, M., Rutten, L., Bu, F., Hartog, M. *et al.* (2018) CRISPR/Cas9-mediated mutagenesis of four putative symbiosis genes of the tropical tree *Parasponia andersonii* reveals novel phenotypes. *Frontiers in Plant Science*, **9**, 284. https://doi.org/10.3389/fpls.2018.00284.

Wang, Q., Hasson, A., Rossmann, S. & Theres, K. (2016) Divide et impera: Boundaries shape the plant body and initiate new meristems. *New Phytologist*, **209**, 485–498. https://doi.org/10.1111/nph.13641.

Wardhani, T.A., Roswanjaya, Y.P., Dupin, S., Li, H., Linders, L., Hartog, M. *et al.* (2019) Transforming, genome editing and phenotyping the nitrogen-fixing tropical Cannabaceae tree *Parasponia andersonii*. *Journal of Visualized Experiments*, **150**, e59971. https://doi.org/10.3791/59971.

Whitford, R., Fernandez, A., De Groodt, R., Ortega, E. & Hilson, P. (2008) Plant CLE peptides from two distinct functional classes synergistically induce division of vascular cells. *Proceedings of the National Academy of Sciences of the United States of America*, **105**, 18625–18630.

Woerlen, N., Allam, G., Popescu, A., Corrigan, L., Pautot, V. & Hepworth, S.R. (2017) Repression of BLADE-ON-PETIOLE genes by KNOX homeodomain protein BREVIPEDICELLUS is essential for differentiation of secondary xylem in Arabidopsis root. *Planta*, **245**(6), 1079–1090.

Yamaguchi, M., Goué, N., Igarashi, H., Ohtani, M., Nakano, Y., Mortimer, J.C. *et al.* (2010) VASCULAR-RELATED NAC-DOMAIN6 and VASCULAR-RELATED NAC-DOMAIN7 effectively induce transdifferentiation into xylem vessel elements under control of an induction system. *Plant Physiology*, **153**, 906–914.

Yang, M.Q., van Velzen, R., Bakker, F.T., Sattarian, A., Li, D.Z. & Yi, T.S. (2013) Molecular phylogenetics and character evolution of Cannabaceae. *Taxon*, **62**(3), 473–485. https://doi.org/10.12705/623.9.

Yaxley, J.L., Jablonski, W. & Reid, J.B. (2001) Leaf and flower development in pea (*Pisum sativum L.*): Mutants cochleata and unifoliata. *Annals of Botany*, **88**, 225–234 https://doi.org/10.1006/anbo.2001.144.

Yevtushenko, D.P. & Misra, S. (2010) Efficient Agrobacterium-mediated transformation of commercial hybrid poplar *Populus nigra* L. × *P. maximowiczii* A. *Henry*. *Plant Cell Reports*, **29**, 211–221. https://doi.org/10.1007/s00299-009-0806-z.

Zadnikova, P. & Simon, R. (2014) How boundaries control plant development. *Current Opinion in Plant Biology*, **17**, 116–125. https://doi.org/10.1016/j.pbi.2013.11.013.

Zhang, B., Holmlund, M., Lorrain, S., Norberg, M., Bako, L., Fankhauser, C. *et al.* (2017) BLADE-ON-PETIOLE proteins act in an E3 ubiquitin ligase complex to regulate PHYTOCHROME INTERACTING FACTOR. *eLife*, **6**, 1–19.

Zhang, H., Lin, X., Han, Z., Wang, J., Qu, L.J. & Chai, J. (2016) SERK family receptor-like kinases function as co-receptors with PXY for plant vascular development. *Molecular Plant*, **9**, 1406–1414.

Zhang, Z., Wang, P., Luo, X., Yang, C., Tang, Y., Wang, Z. *et al.* (2019) Cotton plant defence against a fungal pathogen is enhanced by expanding BLADE-ON-PETIOLE1 expression beyond lateral-organ boundaries. *Communications Biology*, **2**, 238. https://doi.org/10.1038/s42003-019-0468-5.

Zhong, R., Demura, T. & Ye, Z.H. (2006) SND1, a NAC domain transcription factor, is a key regulator of secondary wall synthesis in fibers of Arabidopsis. *The Plant Cell*, **18**, 3158–3170.

Zhong, R., Lee, C. & Ye, Z.H. (2010) Functional characterization of poplar wood-associated NAC domain transcription factors. *Plant Physiology*, **152**, 1044–1055. https://doi.org/10.1104/pp.109.148270.

Zhong, R., McCarthy, R.L., Haghighat, M. & Ye, Z.H. (2013) The poplar MYB master switches bind to the SMRE site and activate the secondary wall biosynthetic program during wood formation. *PLoS One*, **8**(7), e69219. https://doi.org/10.1371/journal.pone.0069219.

Zhu, Y., Song, D., Xu, P., Sun, J. & Li, L. (2018) A HD-ZIP III gene, PtrHB4, is required for interfascicular cambium development in Populus. *Plant Biotechnology Journal*, **16**, 808–817.

Zhu, Y., Song, D., Zhang, R., Luo, L., Cao, S., Huang, C. *et al.* (2019) A xylem-produced peptide PtrCLE20 inhibits vascular cambium activity in Populus. *Plant Biotechnology Journal*, **18**, 195–206. https://doi.org/10.1111/pbi.13187.